Hydrothermal facile Synthesis of Mn-Co-Ni Ternary Metal Oxide Composite with Graphene Nanoplatelets as Electrode Material for Supercapacitor

By

Sarah Malik

School of Chemical and Materials Engineering

National University of Sciences and Technology

2020

Hydrothermal facile Synthesis of Mn-Co-Ni Ternary Metal Oxide Composite with Graphene Nanoplatelets as Electrode Material for Supercapacitor

Name: Sarah Malik

Registration No: Fall 2018-NSE 06, 00000276211

This thesis is submitted as a partial fulfillment of the requirements for the degree of

Master of Science in Nanoscience and Engineering

Supervisor Name: Dr. Iftikhar Hussain Gul

School of Chemical and Materials Engineering (SCME)

National University of Sciences and Technology (NUST)

H-12 Islamabad, Pakistan

2020

Dedication

I dedicate my humble efforts for this exposition and all of my academic achievements to my beloved father, Mr. Muhammad Mutahir Ahmad and my mother, Mrs. Rizwana Kousar who set an example in a way that evolved me to think about character values, strength, composure and determination. These were the values that actually helped me to understand and flourish myself cognitively and personally. My mother who's continues support, motivation, love, inspiration and countless prayers of days and nights make me able to stand at this position to get success and honor. Most importantly my siblings Arooba Malik and Abdullah Mutahir helped a lot for nursing me with devotion, warmth & admiration and are dedicated partners of my success.

Acknowledgement

All praises to Allah Almighty who is the most beneficent and the most merciful. He is the only one who has given me the strength and ability to complete my degree.

I cordially thank to all the people whose assistance was a milestone in the completion of this project.

First of all, I would like to express my deepest gratitude to one of the most important personality **Prof. Iftikhar Gul** who's humble behavior helped me a lot to do my best. It is whole-heartedly appreciated that your great advice and guidelines for my study proved immense towards the success of this study.

I would like to recognize the invaluable assistance of Mr. Mutawara baig and Adeel Akram for giving me expert views and suggestions to make it more dynamic.

I wish to pay special regards to my friends Hadiqa Kayani, Anam Zulfiqar and Mahrukh Ali for their support in my research.

Abstract

Metal oxides and their composites are considered as most promising class of electrode material for future generation supercapacitor. Investigations have revealed that use of Transition metal oxides (TMOs) such as Ru_2O_3, NiO, MnO_2, Fe_2O_3 and Co_2O_3 etc. in supercapacitors yields high specific capacitance, energy density and thermal chemical stability along with environmental compatibility. However, apart from all the development in the field of supercapacitor, limitations like lower energy density, lower capacitive performance of EDLCs, poor life durability of pseudocapacitors and high resistivity lowers their rate capabilities are adversely affecting electrochemical performance. To achieve a higher charge storage capability electrode material with highly accessible surface area and excellent conductivities, carbon material such as graphene, graphene nanoplatelets and carbon nanotubes along with TMO's are used. We have made an effort of synthesizing composite of graphene nanoplatelets with ternary metal oxide of manganese, nickel and cobalt through a simple, facile and cost effective hydrothermal process and further compositional, morphological and electrochemical properties are investigated. Resulting composite of MNC-GNP showed excellent electrochemical properties owing to the high porosity offered by graphene nanoplatelets and synergistic effects produced by individual components of the composite. For comparative studies, ternary oxide MNC was prepared by the same hydrothermal route. XRD confirms the cubic structure of MNC-GNP composite with a crystallite size ranging between 8.66-9.30 nm. SEM showed distinct hierarchical dendritic structures which showed increase in density by the addition of graphene nanoplatelets. Electrochemical testing revealed that MNC-GNP exhibited enhanced supercapacitive behavior with a higher specific capacitance of 1816 Fg^{-1} as compared to MNC which exhibited 1455.5 Fg^{-1} at current density of 2 A/g. GCD also showed increased charge discharge time in the case of MNC-GNP as compared to its counterpart. MNC-GNP has also shown charge stability up to 99.5% of capacity retention up to 1000 cycles. These enhanced electrochemical properties endorse that the synthesized composite can be used as an effective electrode material for supercapacitor

Table of Content

Chapter 1 ……...1

Introduction……..……. 1

1.1 Introduction……..1

1.2 Renewable energy resources ……..2

1.3 Energy storage devices…….……3

1.4 Batteries…….……..…….4

1.5 Fuel cells……..…….6

1.6 Supercapacitors……..…….……...7

1.7 Types of supercapacitor……...……8

1.7.1 Conventional capacitors……..……..8

1.7.2 Electrochemical Double layer capacitor……..….9

1.7.3 Pseudocapacitor……...……..……..…10

1.7.4 Hybrid Supercapacitor……...…….……11

1.8 Electrode Material……..…….……...12

1.8.1 Carbon material…….……..12

1.8.1.1 Activated carbon……..……12

1.8.1.2 Carbon Nanotubes……...…...……...13

1.8.1.3 Graphene ……...…..……..13

1.9 Electrolytes……..……..……14

1.10 Applications of Supercapacitor …….....……14

1.11 Research Motivation ……..14

1.12 Research Objectives ……..…….15

1.13 Research Dissertation ……..…..……15

1.14 Summary ……..……16

Chapter 2 ……..17

Literature Review…….……..…..17

2.1 Emergence of Supercapacitor ……..…….17

2.2 Supercapacitor Principle……..……17

2.3 Types of Supercapacitor ……18
2.4 ECPs based Supercapacitor ……19
2.5 Carbon based composite electrode material……..…..19
2.5.1 Carbon nanotubes as an electrode material……..…….20
2.5.2 Graphene based electrode material…….…..20
2.6 Metal sulfide based supercapacitors ……....……...22
2.7 Activated carbon based supercapacitor ……...….….22
2.8 Metal oxide based supercapacitor ……..……..23

Chapter 3 ……..28

Experimental Section……...…….28

3.1 Synthesis of electrode material…….…….28
3.1.1 MNC…….……28
3.1.2 Process…….……...….29
3.2 Synthesis of MNC-GNP…….……..….30
3.2.1 Process……..…….……...….31

Chapter 4 ……..…..34

Characterization Technique ……..……...……34

4.1 X-ray Diffraction (XRD) ……...…….……...….34
4.2 Scanning electron Microscopy……...….36
4.2.1 Construction of SEM…….……37
4.2.2 Working of SEM……..…….38
4.3 BET surface area analysis ……...…39
4.3.1 Sample Preparation……...…40
4.3.2 Instrumentation…..…….……..……41
4.4 Electrochemical analysis…….…….42
4.5 Cyclic Voltammetry…….45
4.6 Galvanic charge Discharge…….…….46
4.7 Cyclic stability……47
4.8 Electrochemical Impedance Analysis…….……47
4.8.1 Working principle…….47

Chapter 5 …….49

Results and Discussion ……..…...49

5.1 Morphological analysis of nanostructure ……..……..49

5.1.1. MNC ……..……50

5.1.2. MNC-GNP composite……...50

5.2 Phase structural analysis ……..……..51

5.2.1. XRD of MNC …….…….51

5.2.2. XRD of MNC-GNP …….……51

5.2.3. Combined XRD …….…….…….52

5.3 Electrochemical analysis ……..……....……53

5.4 Cyclic Voltammetry …….…….……54

5.4.1. MNC ……..…….…….55

5.4.2. MNC-GNP……..……..56

5.5 Galvanic Charge discharge ……..58

5.5.1. MNC ……..…….58

5.5.2. MNC-GNP …….…….59

5.6 Charge Stability …….…….60

Conclusion ……..……62

References……..63

List of Figures

Figure 1.1: Rangone plot for energy storage devices…….....2

Figure 1.2: Types of energy storage devices……..... 3

Figure 1.3: Comparison of devices……..... 4

Figure 1.4: Comparison of characteristics of energy storage devices..... 5

Figure 1.5: Schematic of working of battery……..... 6

Figure 1.6: Working principle of Fuel cells…… 7

Figure 1.7: types of supercapacitors 8

Figure 1.8: Schematic for working of supercapacitors 9

Figure 1.9: Schematic diagram of working of EDCL supercapacitor.....10

Figure 1.10: Schematic diagram for pseudocapacitors ….....11

Figure 1.11: Schematic diagram for hybrid supercapacitors..... ..12

Figure 1.12: Physical and mechanical properties of Graphene.....13

Figure 2.1: Synthesis of functioning of supercapacitors…….....19

Figure 2.2: Physical properties of Graphene.....20

Figure 2.3: Schematic diagram of manufacture of GNPs from natural graphite ……....21

Figure 3.1: Synthesis of MNC …..... 30

Figure 3.2: Synthesis of MNC-GNP……..…….....33

Figure 4.1: Components of XRD …… 35

Figure 4.2: Possible emissions in SEM operation 38

Figure 4.3: Schematic diagram of SEM.. 38

Figure 4.4: JOEL JSM-6490LA present at SCME;…….….. 38

Figure 4.5: Gemini® VII 2390 Micro porosity analyzer.....42

Figure 4.6: Electrochemical workstation electrodes assembly.....43

Figure 4.7: Electrochemical workstation in SCME.....44

Figure 4.8: CV curves for (a) Ideal case (b) EDLC (c) pseudocapacitor ...45

Figure 4.9: GCD curves for (a) EDLC (b) pseudocapacitor 47

Figure 4.10: EIS (a) Equivalent circuit Diagram (b) Nyquist plot….....48

Figure 5.1: (a) SEM image for MNC at low resolution (b) and (c) SEM image at high resolution ……..……...……50

Figure 5.2: SEM images of MNCO-GNP at different resolutions (a) X=5000 (b) X=10000 (c) X=20000 …….……51

Figure 5.3: XRD analysis of MNCO…….52

Figure 5.4: XRD analysis of MNCO-GNP…...…….53

Figure 5.5: Comparison of XRD …… …….54

Figure 5.6: CV curves for MNC……...56

Figure 5.7: CV curves for MNC-GNP……. …….…..57

Figure 5.8: GCD curves for MNC…… 59

Figure 5.9: GCD curves for MNC-GNP ……..…….....60

Figure 5.10: Cyclic Stablity ……...…..… 61

List of Tables

3.1: Materials used for the synthesis of MNC….....28

3.2: Materials used for the synthesis of MNC-GNP 31

5.1 Specific capacitance for MNC and MNC-GNP at different charge densities……..……..58

List of Abbreviation

Acronym	Meaning
GNP	Graphene Nanoplatelets
MNC	Manganese nickel Cobalt Composite
MNC-GNP	Manganese nickel Cobalt graphene Composite
CV	Cyclic Voltammetry
GCD	Galvanic Charge Discharge
HEG	Hydrogen induced exfoliated Graphene

Chapter 1

Introduction

1.1 Introduction

With each passing day, rapid development of industries is observed due to enhanced product demand. In turn, the pressure on energy resources is increasing. This is all due to high growth rate in human population which leads to enormous energy consumption. The current energy resources are unable to meet the need of energy. The petroleum based fuels are majorly used as major energy source for domestic and industrial use. As a result, these fossil fuels such as coal gas and natural oil are depleting. The dependence on these fossil fuels is the prime factor of environmental pollution [1]. Different hazardous gases such as CO_2, NO_x and SO_x produced by the burning of fossil fuels are the root cause of global warming and greenhouse effect. Moreover water and air pollution also affects the life on earth in bad manner. Heavy metals, gases and organic dyes are causing serious health issues. Moreover untreated wastes from industries are also poured into water bodies and in air lowering the quality of water and air making them harmful for humans, plants and animals. So it is a primary need to find the ways to save environment and enough energy pool to meet the energy crisis at the same time.

Use of renewable energy sources are the solution to these problems [2, 3]. Researchers from all over world are working to find efficient ways for energy generation and storage with a secondary advantage of lowering depletion of fossil fuels an environmental pollution. Two methods are basically being applied for energy generation and storage. First is to directly obtain energy from the primary renewable energy sources i,e sun, ocean waves or air current movement and second is to fabricate devices which are efficient, cost effective and environmental friendly. Fuel cells, solar cells and photo catalysts are used for direct conversion of renewable energy into fuel and electricity [4,5]. Energy storage devices include batteries such as lithium ion batteries, zinc ion batteries and sodium ion batteries, capacitor and supercapacitors [6, 7]. Supercapacitors are gaining a lot of attention due to high power density, cost

efficiency and good life durability [8]. Due to these properties, supercapacitors have vast application, from portable electronics to hybrid electric vehicles and many others.

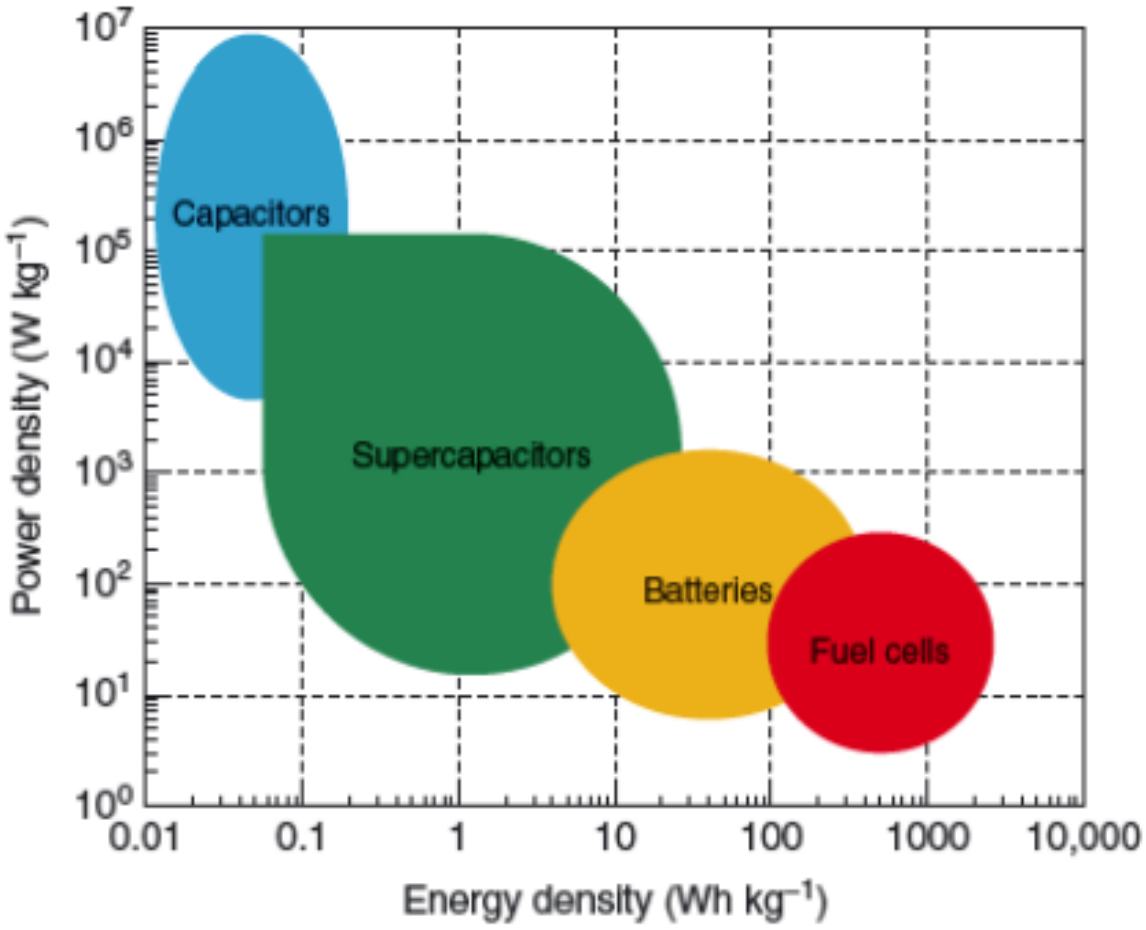

Figure 1.1 Rangone plot for energy storage devices [9]

1.2 Renewable Energy Resources

Renewable energy resources are those resources which are reusable and do not undergo depletion. In contrast to non-renewable energy resources, these resources are environmental friendly and cost effective. With advancement in technology, these resources are considered more promising due to their reusability and cost efficiency.

Renewable energy has many forms which include

- Solar energy [10], [11]
- Wind energy [12]
- Hydrothermal energy [13]
- Geothermal energy [14]

- Biomass [15],[16]

1.3 Energy Storage Devices

With increase in demand, many devices have been fabricated and developed to generate and store energy. Different type of energy systems are included such as

- Chemical system
- Electrical system
- Electrochemical system
- Mechanical system
- Thermal system [17]

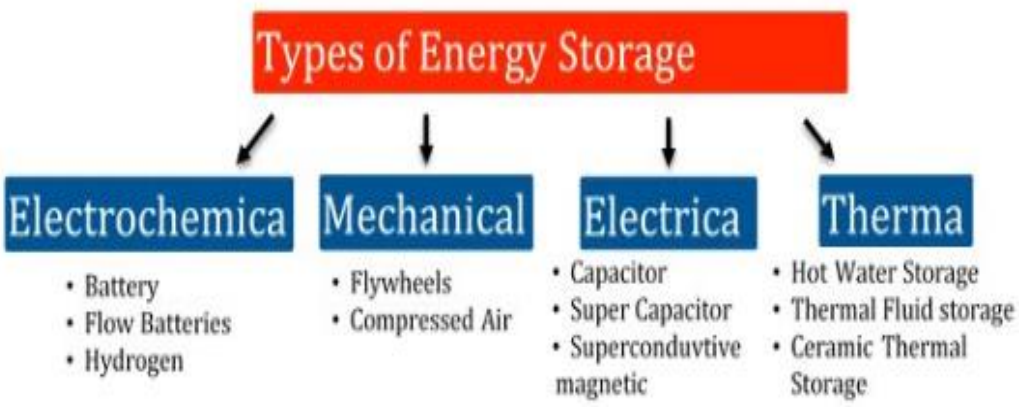

Figure 1.2 Types of energy storage devices

Electrochemical and electrical devices are most commonly used. These include batteries, capacitors and supercapacitor.

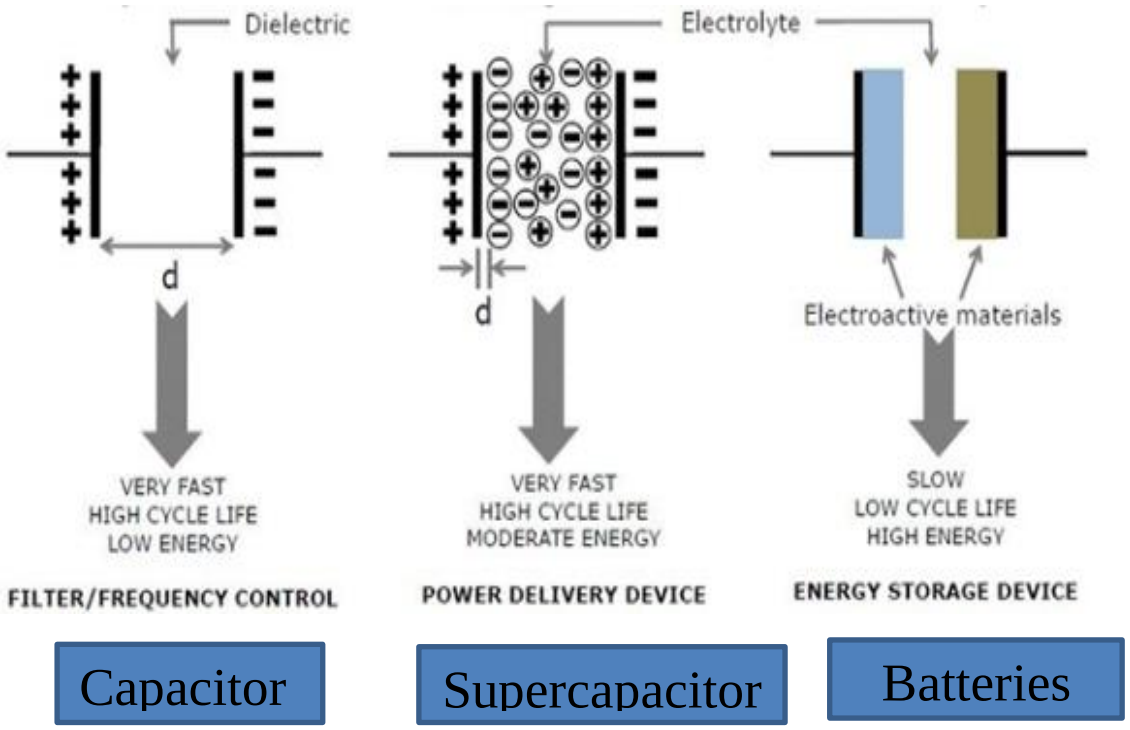

Figure 1.3 Comparison of devices

1.4 Batteries

Battery is a device that converts chemical energy into electrical energy through a reversible electrochemical reaction and stores energy or supplies it to another power consuming device.

Characteristics	Capacitor	Supercapacitor	Battery
Specific energy ($W\,h\,kg^{-1}$)	< 0.1	1–10	10–100
Specific power ($W\,kg^{-1}$)	$\geq 10,000$	500–10,000	< 1000
Discharge time	10^{-6} to 10^{-3}	s to min	0.3–3 h
Charge time	10^{-6} to 10^{-3}	s to min	1–5 h
Coulombic efficiency (%)	About 100	85–98	70–85
Cycle-life	Almost infinite	$> 500,000$	about 1000

Figure 1.4 Comparison of characteristics of energy storage devices [18]

Different type of batteries include

1) Primary batteries:

   These batteries have a lifetime of one cycle and can be chargeable for one time only. They have their application mostly in portable devices. Primary batteries can be classified on the basis of nature of electrolyte used in them. For example: Aqueous and non-aqueous electrolytes, both are used in primary batteries.

2) Secondary batteries:

   These batteries are chargeable for more than one time. Applications of secondary batteries can be found in vehicles, portable electronic devices, solar cells etc. -secondary batteries are classified further on the basis of types of electrodes.

   - Lithium ion batteries
   - Sodium batteries
   - Lead acid batteries
   - Lithium sulphur batteries
   - Lithium Polymer batteries

Batteries have high energy density, low power density, rechargeable but have slow cycle rate.

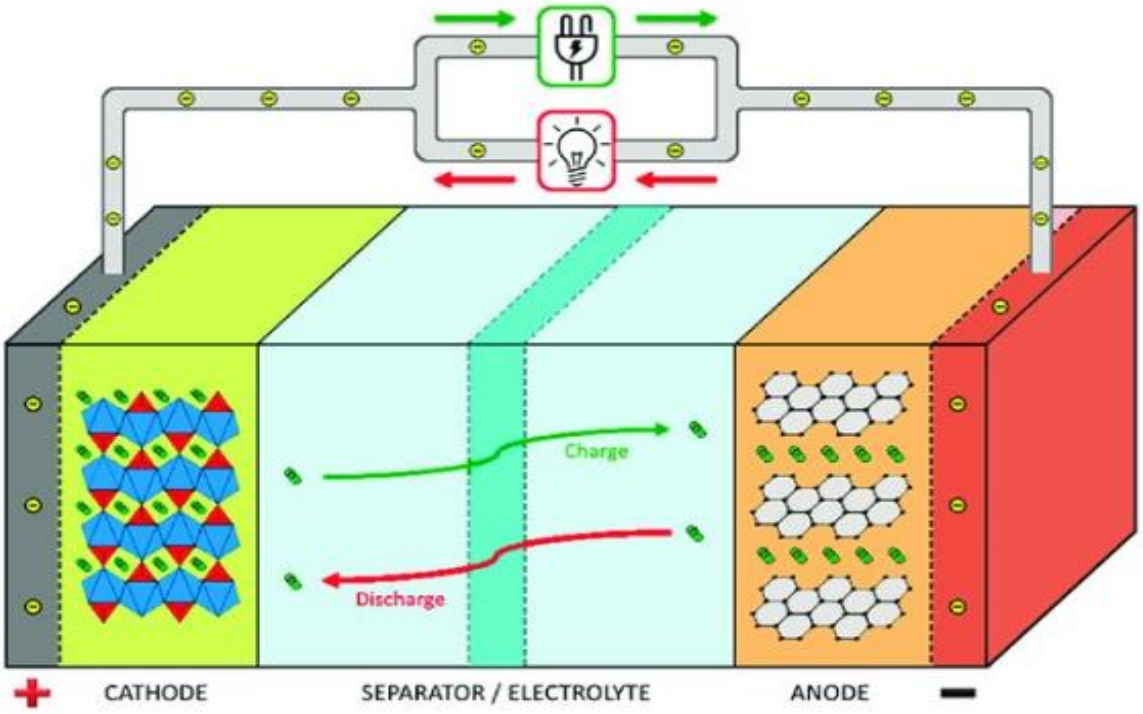

Figure 1.5 Schematic of working of battery [19]

1.5 Fuel Cells:

Fuel cells not only store energy but also generate energy. Fuel cells undergo a number of chemical redox reaction occurring between any oxidizing agent and fuel and generate energy. Fuel cells are composed of three components including electrolyte. Electrolyte is involve in transferring ions between electrodes during a chemical redox reaction. Most commonly used electrolytes are Potassium hydroxide, acid and other salts.

Different types of fuel cells include

- Phosphoric acid fuel cell
- Solid oxide fuel cell
- Polymer exchange fuel cell
- Alkaline fuel cell
- Molten carbonate fuel cell

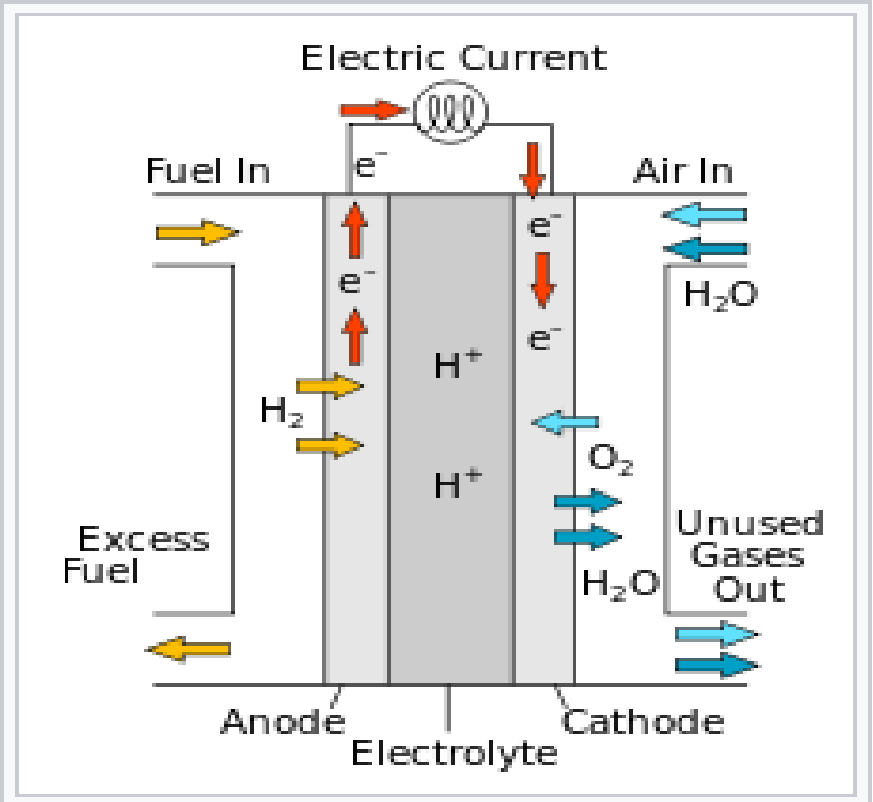

Figure 1.6 Working principle of fuel cell

1.6 Supercapacitor

Supercapacitors, also known as electrochemical capacitors, are gaining lots of attention from decades due to their cost efficiency, high power density, long cycle life time and fast charge discharge rates. Due to these properties, supercapacitors have vast application, from portable electronics to hybrid electric vehicles and many others.

Supercapacitor consist of two electrodes separated by an insulating material called dielectric. Working principle of supercapacitor is that when potential is applied across the electrodes, charge began to accumulate on electrodes.

Specific capacitance is given by

$$\mathbf{Q = CV}$$

Where C is specific capacitance

V is operating window

Q is charge stored

There are following types of supercapacitor depending upon storage mechanisms used to store energy.

1) Conventional Capacitors
2) Electrochemical double layer capacitor
3) Pseudocapacitor
4) Hybrid capacitors

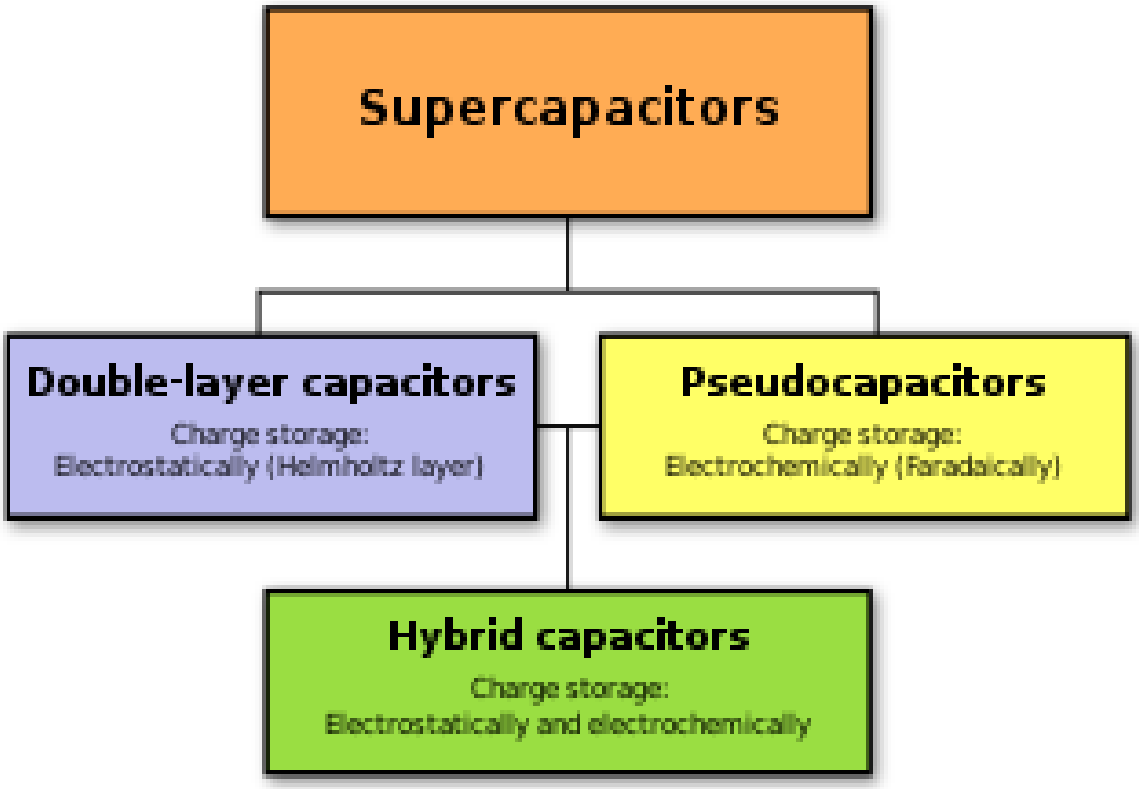

Figure 1.7 Types of supercapacitor

1.7 Types of Supercapacitor

1.7.1 Conventional capacitors

Capacitor is an energy storing device which consists of two electrodes separated by an insulating material called dielectric. When voltage is applied, one electrode gain positive charge while other gets negative. Both electrodes accumulate charge of equal

magnitude. The ability of a capacitor to store energy is called capacitance. It is measured in Farad.

$$C = \frac{A\varepsilon}{4\pi d}$$

It is given as

Here

A = Surface area

Ɛ = Dielectric constant

d = separation distance

Energy accumulated by conventional capacitors is about microfarad and picofarad.

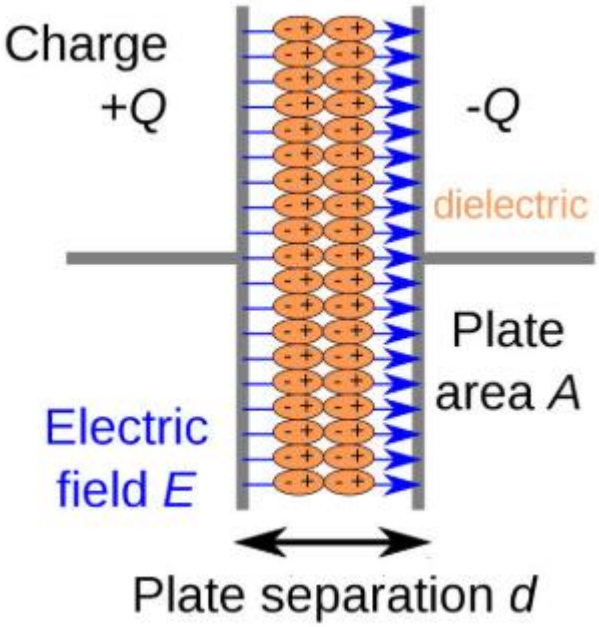

Figure 1.8 Schematic of working of supercapacitor [20]

1.7.2 Electrochemical Double Layer capacitor

EDLC utilizes electrode-electrolyte interface. Electrical energy is stored by charge accumulation mechanism. Due to this mechanism, EDLC differ from conventional capacitor that utilizes dielectric material for charge storage. In EDLC, the electrode material's surface is very effective. In order to endure charge on interface, a large

surface area helps the maximum contact between active material and electrolyte. In charging process of EDLC, the effect of external applied potential difference, the electrons move from cathode to anode and cation move from anode to cathode. During discharging process, electrons move in opposite direction i.e. from anode to cathode. Common materials used in EDLC are carbon based such as graphite powder, MWCNTs, SWCNTs, activated carbon and graphite etc. No chemical redox reaction in involved in this type of supercapacitors

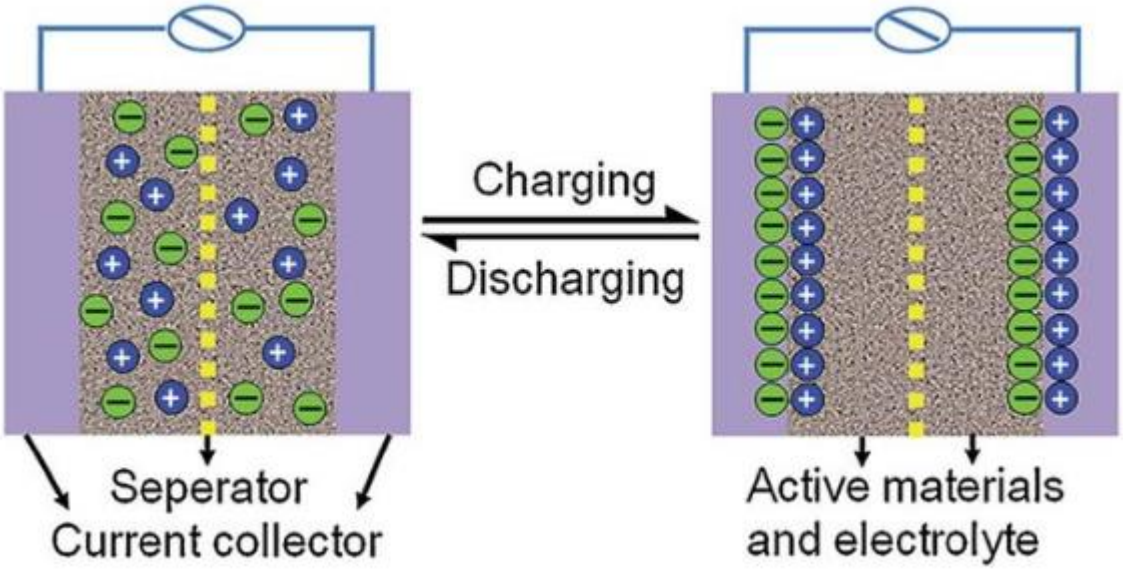

Figure 1.9 Schematic of working of EDLC [21]

1.7.3 Pseudocapacitor

Working principle of this kind of supercapacitors is to store charge via redox reactions. These redox reactions occur at the interface of active material [22, 23]. The material for electrodes of supercapacitor is selected on the basis of ability to betray redox reaction.

A vast variety of material is being used for electrodes of pseudocapacitors such as organic polymers (polyaniline and polypyrrole), metal oxides (NiO, Co_3O_4, CuO and $NiCo_2O_4$ etc) and metal sulphides (MoS_2) etc.

Merits

1. Pseudocapacitors contain high charge density and large specific capacitance.

2. They are cheap in cost.

Demerits

1. Their rate capability is low
2. Low life durability

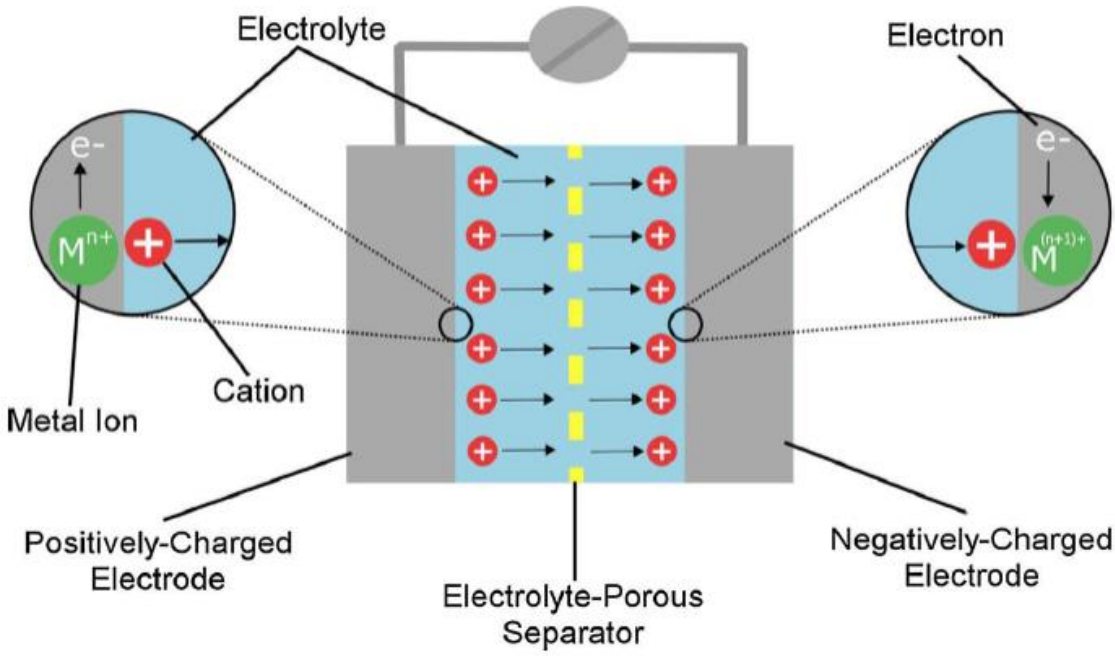

Figure 1.10 Schematic of pseudocapacitor [24]

1.7.4 Hybrid Supercapacitor

This type of supercapacitor is the combination of pseudocapacitor and EDLC, that is why, is called hybrid supercapacitor. It contains both pseudocapacitor and EDLC as positive and negative electrodes respectively. Both electrodes are separated by a semipermeable film which behaves as separator in order to isolate both electrodes from electrical contact. An electrolyte solution is impregnated on electrodes and separator and allows the flow of ions between electrodes and stop electrode from discharging the cell.

Characteristics

1. Hybrid supercapacitors have excellent specific capacitance.
2. They have high energy density.

3. Good cyclic stability.

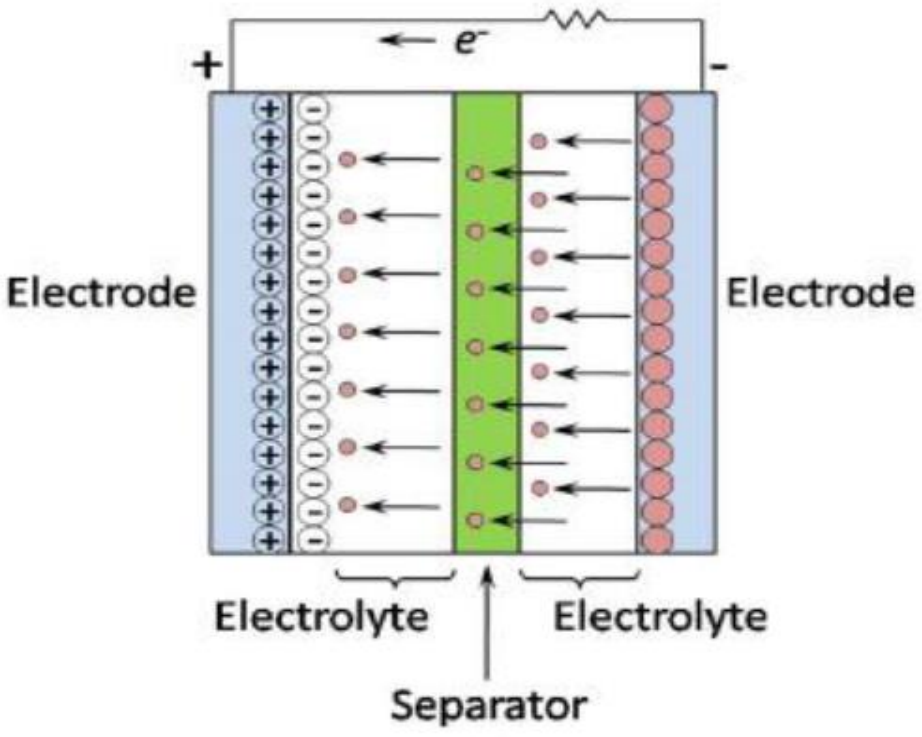

Figure 1.11 Schematic of hybrid supercapacitor [25]

1.8 Electrode materials

Nanostructured materials have resulted into high-performance supercapacitors. Surface area is a key part of material as it greatly affects capacitive performance. Owing to the high porosity and pore volume of nano-materials result into the high capacitance of the material. Following are the three major types of electrode materials.

1.8.1 Carbon based material

Due to proficiency of processing, cost effectiveness and high abundance, the carbon materials classified as:

- **1.8.1.1 Activated carbon**

In comparison to carbon nanotubes and graphene, activated carbon has high surface area and are less expensive. That is why it is widely used for super capacitors. It is

obtained from natural resources. Carbonization process, a heat treatment process under an inert atmosphere, activates the precursors.

- **1.8.1.2 Carbon nanotube (CNTs)**

Carbon nanotubes (CNTs) provide wide applications for super capacitors by decomposition of hydrocarbons. SWCNTs and MWCNTs can be synthesized depending upon different process. CNTs shows high surface area and high conductivity. Their chemical as well as mechanical properties are excellent. Supercapacitors made from CNTs utilizes the maximum surface area in order to show the maximum capacitance.

- **1.8.1.3 Graphene**

Due to superior properties of high-performance energy applications, researchers are heavily focusing on graphene from past few decades. Graphene possesses large surface area (2675$m^2 g^{-1}$) and exceptional conductivity (6000 Scm^{-1}) [26]. These are light weighted, efficient and cost effective. Due to greater charge mobility, it provides good capacitance

Property	Graphene	Ref
Electron mobility	1500 $cm^2 V^{-1} s^{-1}$	[14]
Resistivity	$10^{-6}\Omega$-cm	[14]
Thermal conductivity	$5.3 \times 10^3 Wm^{-1}K^{-1}$	[14]
Transmittance	>95% for 2nm thick film >70% for 10nm thick film	[15]
Elastic modulus	0.5 – 1 Tpa	[15]
Coefficient of thermal expansion	-6×10^{-6}/K	[15]
Elastic modulus	0.5 – 1 Tpa	[15]
Specific Surface area	2630$m^2 g^{-1}$	[16]
Tensile strength	130 GPa	[16]

Figure 1.12 Physical and Mechanical properties of Graphene

1.9 Electrolytes

The performance of supercapacitor is greatly affected by the type of electrolyte used. The flow of charge depends on the concentration of ions. The performance of device reduces if concentration of electrolyte is below 0.2M.

Following are different types of electrolytes used in supercapacitors.

Acidic electrolyte:

- Hydrochloric acid
- Sulphuric acid

Basic electrolyte:

- Potassium Hydroxide
- Sodium hydroxide
- Potassium chloride

Gel-polymer electrolyte:

- PVA-KOH gel electrolyte

1.10 Applications of Supercapacitor

Supercapacitors are widely used in

- Consumer electronics
- Grid stabilization
- Railway system
- Hybrid transportation
- Automobile industry [27]

1.11 Research Motivation

Apart from all the development in the field of supercapacitors, limitations like lower energy density, lower capacitive performance of EDLCs and poor life durability of

pseudocapacitors are still present. Research in arena of material science with aims of finding materials that can link the gap between supercapacitors and batteries are vital.

Investigations are held in order to find the retarded life cycle of pseudocapacitors revealed the low performance of active material.

The performance of the device is also hindered due to localization of the charge transfer process to the surfaces of nanomaterials especially in the case of inorganic material [28].

The combination of binary or ternary metal oxides with carbon material can result into a better active material for excellent pseudocapacitive and EDLC performance.

1.12 Research Objectives

The basic objective of our research is to develop a material with can meet the problems confronted in the field of supercapacitors. Major goals of research are

- The exploitation of pseudocapacitance of transition metal oxides and their composites.
- Designing an adequate approach to check capacitance and durability of materials with carbonaceous origin.
- Synthesis of ternary transition metal oxides and their nanocomposites

1.13 Dissertation Organization

Thesis comprises of following sections;

Chapter 1:

It gives the main idea of the work and motivation of selection of topic. It also gives an idea about the objective of the research.

Chapter 2:

This chapter includes the insight of gradual development in the field of super capacitors, its types with respect to electrode material and literature reviews about the progressing work. This chapter also gives an adequate approach to overcome the challenges in the field of supercapacitors.

Chapter 3:

This chapter gives a comprehensive review of the synthesis route followed for the synthesis of transition metal oxides and graphene nanoplatelets composite.

Chapter 4:

Characterization techniques and testing methods that are applied are discussed in this chapter

Chapter 5:

Results obtained by the characterization techniques (such as SEM, XRD, IR and BET) and testing methods (such as CV analysis, GCD) are discussed in this chapter.

This chapter provides the conclusion of the research and the objectives that are achieved during the reseach.

1.14 Summary

This chapter gives the introduction of different energy storage devices that are used now a days. It also demonstrate the state of these devices such as batteries, fuel cells, capacitors and supercapacitors with their working and merits and demerits. This chapter also illustrates the motivation of selection of the topic and objective of conducting the research. In the end, the organization of the research is given.

Chapter 2

Literature Review

2.1. Emergence of Supercapacitor

170 years ago, the understanding of electricity at the molecular level was started. With the advent of Leyden jar in 1946 by Dean Kleist and Kamin Pomerania concurrently at Leyden in Netherland, investigations were done for deep understanding on charge storage and charge separation mechanisms on the surface of jar with glass separation. The device was firstly named as “Condenser” and it was changed to “capacitor” later. Its charge storage ability was called “capacitance” [29]. Becker was the one awarded with the first patent in the field of supercapacitor research in 1957 [30]. SOHIO established the first energy storage device by using carbon based materials as electrode and tetra-alkyl ammonium salt as electrolyte in 1969 [31]. First successful double layer capacitor with title “supercapacitor was presented by Nippon electric company in 1971. These supercapacitor had high internal resistance due to low voltages and had application in memory backup and many other consumer appliances. BE Covey and his coworkers had made a great contribution in the field of supercapacitors during 1970s and 80s by working on ruthenium oxide based energy storage devices which yielded high capacitive behavior due to low internal resistance[32].

.In 90s, hybrid electic automobile supercapacitors gained a lot of attention. A huge amount of research was done on supercapacitors and a good number of patents was also granted. The commercial production of supercapacitor in the ongoing markets is based on highly porous carbonaceous material exhibiting high surface area and transition metal oxide system. These commercial applications were used in telecommunication equipment, circuits, memory devices and activators etc.

2.2. Supercapacitor Principle

A supercapacitor comprises of two oppositely charged electrodes separated by dielectric material sunk into an electrolyte. It also possesses current collectors. The

energy storing ability of a supercapacitor is linked with the property of electrodes to accumulate and distribute collected charges [33]. For a capacitor having two electrodes having an area A, separated by a distance d in a parallel configuration in vacuum,

Capacitance is given by Eq 2.1

$$C = \frac{A}{4\pi d}$$

If dielectric medium with permittivity Ɛ is present as a separator then capacitance is given by equation 2.2

$$C = \frac{A\varepsilon}{4\pi d} \qquad (2.2)$$

The energy density W, of a supercapacitor is given by equation 2.3

$$W = \frac{1}{2} CV^2 \qquad (2.3)$$

Here C represents capacitance and V represents voltage.

2.3. Types of Supercapacitor

There are many categories of supercapacitors based on type of active material used including Transition metal oxides and sulfides MoO_3, RuO_3, MnO_2, WO_3, Co_3O_4, NiO, Fe_2O_3 as well as MnS, CuS, Ni_3S_2, ZnS and Al_2O_3 [34-43]. Electrically conductive polymers (ECPs) including polythiophene, polyanaline and polypyrrole, their composite and derivatives with metal oxides are used in supercapacitors.[45-50]. Other carbon based materials such as carbon nanotubes, graphene, graphene nanoplatelets, carbon aerogels and composites of these materials with metal oxides and metal sulfides [50-53].

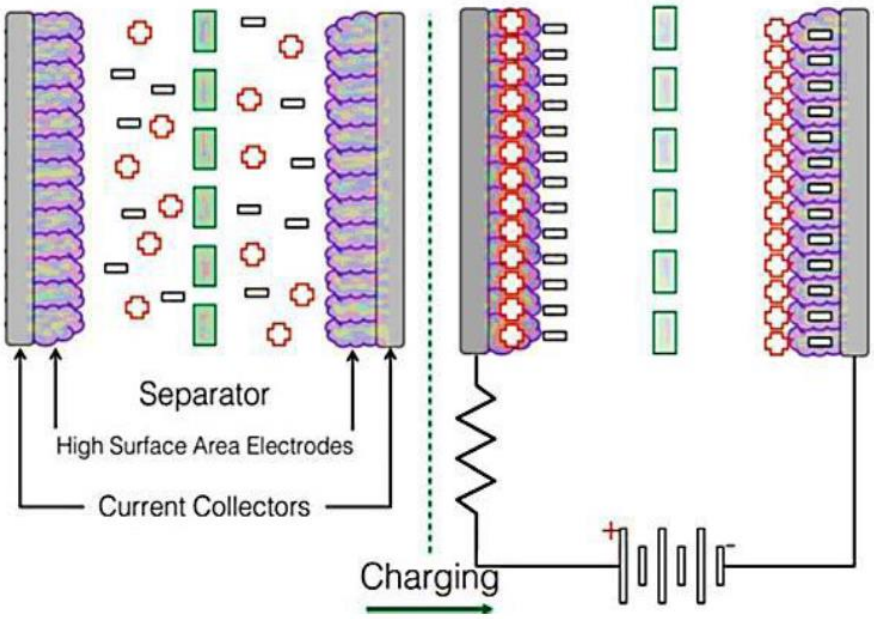

Figure 2.1 Schematic of functioning of supercapacitors [33]

2.4. ECPs based Supercapacitors

ECPs consist of conjugated systems due to which electron can travel along the polymer's backbone. This is the reason of electrical conductance of polymers. Extensive investigations are being done on ECPs during past two decades due to their cost effectiveness, high charge density and their faradaic reversibility [54]. Different morphological varieties like bulk powder, nanowalls, nanosheets and nanorods have paved the way towards flexible capacitors. Good capacitive performance is shown by nano structured ECPs due to high porosity and high surface area. Polythiophene, polyanaline, polypyrrole, their composite and derivatives with metal oxides are used in supercapacitors due to low cost, high thermal stability, fast charge discharge rate and excellent energy storage capacity. Each ECP show different properties and can be used according to the application need.

2.5. Carbon based composite electrode material

Many derivatives of carbon based materials such as CNTs, carbon aerogels, graphene, GNPs and activated carbon used as electrode material in supercapacitors. Composites nanostructures of carbon with other polymers, metal oxides and metal sulfides are used.

2.5.1 Carbon nanotubes as an electrode material

Carbon nanotubes are an allotropic form of carbon having its dimension in nano scale. Extensive investigations are being done on CNTs to be used as electrode material for EDLCs due to high mechanical strength and conductivity. Single walled and double walled carbon nanotubes, both are extensively used in the field of supercapacitor in order to increase electrical conductance and mechanical strength.

2.5.2 Graphene based electrode material

Unique properties of graphene like one atom thick 2D structure, high mechanical strength, high conductivity, high surface area and innate flexibility makes it the intensively used material for investigations regarding supercapacitor [55]

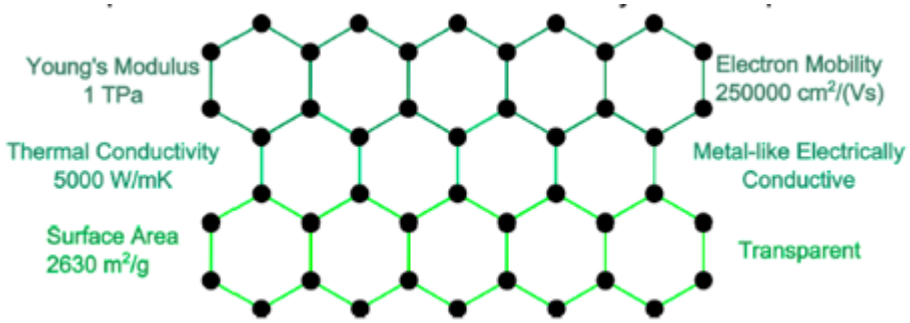

Figure 2.2 Physical properties of graphene [56]

Graphene covers all kind of graphitic material ranging from 100 nm <thick platelets down to single layer graphene.

Graphene is considered to be a good reinforcement material because of greater ability to transfer the stress. Hence mechanical strength is increased. Intense efforts have been done to find out better methods of synthesizing graphene and its derivatives for research purposes. Different methods are presented till now for the synthesis of graphene such as mechanical cleavage, chemical vapour deposition (CVD), acid irradiation of graphite, ball milling and sonication.

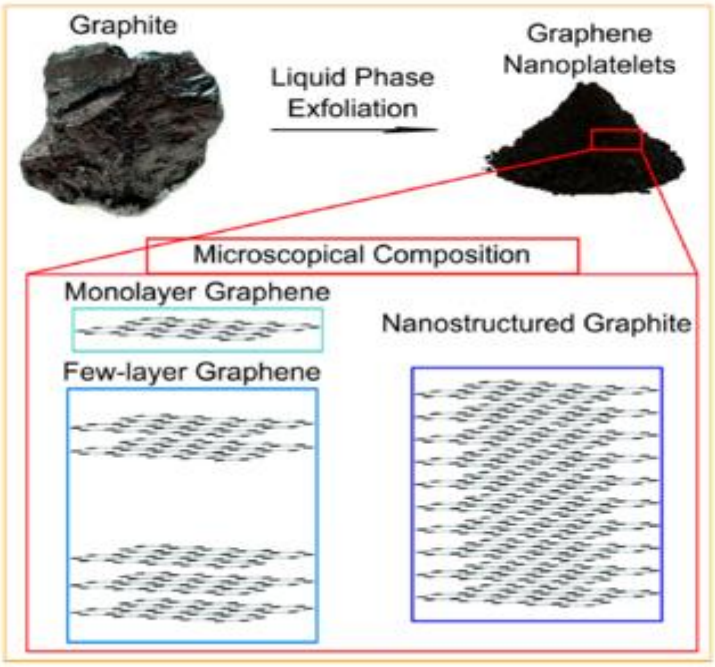

Figure 2.3 Schematic of manufacture of GNPs from natural graphite [56]

Graphene nanoplatelets are simply comprised of small stacks of graphene. GNPs can replace the carbon nanotubes as the possess properties similar to carbon nanotubes [57]. Graphene nanoplatelets have lesser tendency to twist which reduce the performance of CNTs. This property make GNPs more dispersible into the matrix in turn increasing surface area, mechanical strength and stiffness. Advantage of GNPs on other allotropes of carbon is these are less costly and less hazardous to health. The intrinsic properties of graphene have made them useful for a wide range of applications such as batteries and supercapacitors. GNPs are used as nanoscale additives in composites for synthesis of conductive electrodes, coatings, adhesives and as components of e-inks. As reinforcement material, GNPs are found to be promising material to be used in aeronautical, aerospace and automobile industry.

Metal graphene composites are intensively being studied due to excellent mechanical properties and good bonding between graphene and matrix. Inspite of good results by researches, still there are some challenges to address such as dispersion of graphene into metal matrix as there exists density difference between graphene and metal matrix etc.

2.6 Metal sulfide based Supercapacitors

Metal sulfides and their composites are of strong interest leading to their excessive use electrode material for commercially applied supercapacitors [58-60]. Pseudocapacitive behavior of metal sulfide based electrodes resulting from faradaic chemical reactions gives them advantage over carbon based supercapacitors. The carbonaceous material have charge storage mechanism which is based on charge storage confined to the active area of electrode. Many researches are being done due to superior electronic as well as electrochemical performance which showed higher capacitance and long life such as R.B. Pujari have reported specific capacitance of 747 Fg^{-1} at 1 $mAcm^{-2}$ on MnS microfiber on the stainless steel as the substrate[61]. X.F. synthesized nanostructured nickel cobalt sulfide deposited on the nickel foam as electrode material for supercapacitor with high capacitance of 2068 Fg^{-1} capacitance at 5 $mAcm^{-2}$ current density [62].

Excessive capacitive loss and short life cycle of metal sulfide based electrodes adversely affects its electrochemical performance. Volume induced structural variations and excessive capacitive loss over prolong cyclic life are the major drawbacks in the success of metal sulfides based electrodes. Moreover exploration of other economically acceptable and highly redox metal oxide based electrode material for commercial application of supercapacitor is crucial. Many solutions to this problem is proposed by the researches such as using their composites with ECPs and other carbon based materials.

2.7 Activated carbon

Owing to their low prices, large surface area and good electrical properties, activated carbons are also being used in researches as electrode material in supercapacitors. Activated carbon possess large surface area up to 3000 m^2/g depending upon the used precursor and stimulation approach [63-66]. Chemical and physical stimulation of carbonaceous matter such as coal, nutshell, wood etc. is done for the formation of activated carbon. Physical stimulation means the use of carbon matter at the temperature range between 750-1200^o C. Chemical stimulation generally done at low ranges 410^o-710^o C.

A wide pore size range of ACs with micro(less than 2nm), marco (2-50nm) and meso (more than 50nm) sizes is obtained from both physical and chemical stimulation. Investigations involving ACs as electrodes revealed that high porosity is not the only sufficient parameter for high performance of storage devices as capacitance of 10 F/g for an area of 3000cm^{-2} was obtained. Homogeneous pore size distribution, pore shape and surface specificity can also affect the performance of AC electrode. Moreover, electrochemical performance of the electrode is reduced because of moisture and acidic functional sites on the surface of AC [67]. Wettability of the carbon surface by the electrolyte is also an important factor affecting the performance of the supercapacitor. Liquid electrolytes offer much higher capacitance (100-300Fg^{-1}) than organic electrolytes (around 150 Fg^{-1}) [68]. ACs have been used in commercial production of supercapacitor electrode. Although their application as a successful electrode material is still limited due to appropriate surface functionalities and proper pore size engineering.

2.8 Metal oxide based Supercapacitors

Metal oxides and their composites are of strong interest these days leading to their excessive use electrode material for commercially applied supercapacitors [58-60]. Pseudocapacitive behavior of metal oxide based electrodes resulting from faradaic chemical reactions gives them advantage over carbon based supercapacitors. The carbon based materials have charge storage mechanism which is based on charge storage confined to the active area of electrode.

Hu et al. in 2014 synthesized hierarchical Co_3O_4@MnO_2 for energy storage by facile hydrothermal method on Ni foam. Its specific capacitance was 560 Fg^{-1} at 0.2 Ag^{-1} and 95% capacitance retention after 5000 charge-discharge cycles. Moreover asymmetric device was assembled with GO and achieved energy density of 17.7 $Whkg^{-1}$ at power density of 158 $kWkg^{-1}$ [69]

Liuyang Zhang et al. prepared a series of binary compounds of nickel copper oxide synthesized directly upon flexible light weight carbon fibre paper substrate as binder free electrodes. They achieved highest specific capacitance of 1711 Fg^{-1} at a higher discharge current density of 5 Ag^{-1}[70]

J.L. Yin et al. synthesized micro branched copper/nickel oxide composite by using two simple and continuous electroplating processes, chemical oxidation and annealing process. Maximum measured specific capacitance was 296.2 F/g at a scan rate of 10 mV/s. This composite also exhibited long cycle life with 97% specific capacitance retained after 500 cycles [71]

Excessive capacitive loss and short life cycle of (MOx) based electrodes adversely affects its electrochemical performance. Volume induced structural variations and excessive capacitive loss over prolong charge-discharge cycles are the significant challenge in the success of (MOx) based electrodes. Moreover exploration of other economically acceptable and highly redox metal oxide based electrode material for commercial application of supercapacitor is crucial. Many solutions to this problem are proposed by the researches such as using binary or ternary metal oxides systems and their composites with ECPs and other carbon based materials.

Literature review about the electrochemical performance of the supercapacitor has revealed that the metal oxide based electrode material have high pseudo capacitance but limitations like excessive loss of capacitance over prolong charge discharge cycles and volume induces structural variation are still big challenges. Short life cycle and excessive capacity loss are observed which affect the electrochemical durability of the transition metal oxide based electrode materials. On the other hand carbon based material have good mechanical strength, electrical properties and good life durability but are limited by low EDLCs performance. Consequently, combining metal oxides with different carbonaceous nanostructures based electrode systems are expected to give good results due to synergistic effect.

Yanhua Li et al. synthesized $MnCo_2O_{4.5}$/Graphene composite through hydrothermal process which gave specific capacitance of 225.6 Fg^{-1} at 1.0 Ag^{-1} and 92.6% initial specific capacitance retention at 1000^{th} cycle [72]

Seung Woo Lee et al. demonstrated that LbL assembled MWCNT/MnO_2 thin film electrode yield high volumetric capacitance of 246 F/cm^3 with a good capacity retention of 1000 mV/s [73]

Xianfu Li et al. grew CuS nanoplatelets arrays on graphene nanosheets through solvothermal process at low temperature. Graphene/CuS electrode delivered a high capacitance of 497.8 Fg^{-1} at high current density of 0.2 Ag^{-1} [74]

Asish kumar Mishra et al. synthesized graphene via Hydrogen induced exfoliation and it was further functionalized with metal oxide nanoparticles and polyanaline via chemical routes. Maximum specific capacitance observed for different nanocomposites were 80 F/g for HEG, 125 F/g for f-HEG, 265 F/g for RuO_2-f-HEG, 60 F/g for TiO2-f-HEG, 180 F/g for Fe3O4–f-HEG and 375 F/g for PANI–f-HEG obtained with 1M H2SO4 as electrolyte at voltage sweep rate of 10mV/s with 85 percent capacitance retention for each nanocomposite [75]

S. L. Chiam et al. reported a method of enhancing energy density of a device through the parallel stacking of five copper foils coated on each side with graphene nanoplatelets. It yielded optimum specific energy density of 24.64 Wh/kg and specific power density of 402 W/kg at 0.8V [76]

Huanlie Wang et al. synthesized graphene-nickel cobaltite nanocomposite as positive electrode which showed significantly higher capacitance of 618 F/g than graphene-Co_3O_4 (340 Fg^{-1}) and graphene-NiO (375 Fg^{-1}) prepared with the same method [77]

Ashutosh K. Singh et al. reported a facile method to prepare Co_3O_4-MnO_2-NiO ternary hybrid 1D nanotube arrays for their application as active material for high performance supercapacitor electrodes. It yielded specific capacitance ~2525 F/g with 80% retention of specific capacitance after 5700 successive cycles [78]

S. Jayasubramaniyan et al. prepared $Mn_{1/3}Ni_{1/3}Co_{1/3}MoO_4$ and $Mn_{1/3}Ni_{1/3}Co_{1/3}MoO_4$ dispersed in various percentages of reduced graphene oxide composites via hydrothermal method. Specific capacitance of 1750 F/g at 1Ag^{-1} with a cyclic efficiency of 85.5% after 5000 cycles at 10 Ag^{-1} was obtained [79]

Highly flexible solid state fiber supercapacitor was fabricated by Yaqiang Ji.et al. by binder free integrated electrodes of hierarchical $MnCo_2O_4$ nanothrowns grown on porous nickel bilayer coated Cu-wires. The fiber supercapacitor showed capacitance of 54.8 mF/cm^2 with energy density of 12.8 $\mu Whcm^{-2}$ at power density 110 μWcm^{-2} . Good rate capability and cycling capability was observed [80].

Chang Chen et al. synthesized cubical spinal $MnCo_2O_4$/graphene sheet (MCO/GS) nanocomposites via hydrothermal method for application as anode material for lithium ion batteries. It exhibited high reversible discharge capacities of 1350.4 $mAhg^{-1}$ at the initial rate of 100 mAg^{-1} , excellent rate capability of 462.1 $mAhg^{-1}$ at a current rate of 4000 mAg^{-1} and outstanding cycling performance of 584.3 $mAhg^{-1}$ at 2000mAg^{-1} after 250 cycles. It also showed promising electrochemical properties as anodic material for sodium ion batteries [81].

Shaymaa Al-Rubaya et al. prepared $MnCo_2O_4$/Graphene nanoplatelets composite which showed a high specific capacitance of ~1268 Fg^{-1} at 1mVs^{-1} scan rate with a current density of 7.81 Ag^{-1} [82].

Yufeng Zhao et al. synthesize monolayer nickel cobalt hydroxyl carbonate for high performance All-solid-state asymmetric supercapacitor which resulted in a high specific capacitance of 2266 Fg^{-1} and promising energy density of 50 $Whkg^{-1}$ and power density of 8.69 $kWkg^{-1}$ [83].

Liang Huang et al. in 2013 reported a high capacitance of ~1.64 F/cm^2 at 2 mA/cm^2 of nickel-cobalt hydroxide nanosheets coated on $NiCo_2O_4$ nanowires grown on carbon fiber paper for high performance pseudocapacitor, with excellent rate capability, specific energy density (~33Wh/kg), power density (~41.25 kW/kg) [84].

Xu Wang et al. synthesized highly conductive nickel cobalt oxide single wall carbon nanotube (Ni-Co_2O_4-SWCNT) nanocomposite for high performance supercapacitor application which exhibited high capacitance of 1642 Fg^{-1} with excellent cycling stability of 94.1% retention after 2000 cycles [85].

Lu Li et al. synthesized spinal manganese-nickel-cobalt ternary oxide nanowire arrays on Ni foam via hydrothermal synthesis to be used as positive electrode in supercapacitors. It showed specific capacitance of 638 Fg^{-1} at 1 Ag^{-1} and excellent cycling stability when applied in asymmetric supercapacitor [86]

Zhang et al. in 2013 synthesize hierarchical nanowires of Co_3O_4@$NiCo_2O_4$ for supercapacitor. It exhibit high aerial capacitance of 2.04 F/cm at 5 mVs^{-1} and 83.7% capacitance retention after 1500 cycles [87].

Basic objective of this research is to design an adequate approach to develop an active material that has better electrochemical performance with cost efficiency and better life durability. So I opted to exploit the pseudocapacitive nature of ternary transition metal oxides and good durability of GNPs in order to overcome the challenges faced in the field of supercapacitors.

Summary

This chapter gives a brief overview of emergence of supercapacitors over time. Working principle was also explained. Types of supercapacitors based on the different type of electrode materials are explained. Detail about types of electrode materials with their derivatives and some recent research work are given. In the end, literature review about the topic of research topic is given.

Chapter 3

Experimental Section

3.1 Synthesis of Electrode material

3.1.1 MNC

Materials used for synthesis of MNC are listed below

Material name	Purity level	Company name
Cobalt nitrate hexahydrate	99%	Sigma Aldrich
9Manganese nitrate tetrahydrate	99%	Sigma Aldrich
Nickel nitrate hexahydrate	98%	Merck company
Sodium carbonate	98%	Thermo Fisher

Table 3.1 Names of materials used for synthesis of MNC

Instrument used during the process are:

- Teflon lined stainless steel autoclave
- Oven
- Magnetic stirrer
- Hotplate
- Beakers
- Petri dishes
- Weighing balance
- Muffle furnace

3.1.2 Process:

1) The synthetic route followed for the synthesis of MNC is the hydrothermal method. The process for synthesis of MNC is represented in Fig 2.1.

2)1M nickel nitrate hexa hydrate, 1M cobalt nitrate hexa hydrate and 1M manganese nitrate tetra hydrate were measured on a weighing balance and then added in 10ml of deionized water under constant stirring.

3) In another beaker, an appropriate amount of sodium carbonate was added in 60 ml of deionized water under constant stirring to ensure proper dissolution.

4) Then the Na_2CO_3 solution was poured into other metal nitrate solution drop wise under constant stirring.

5) Then this homogeneous solution was transferred into a Stainless steel autoclave and placed in an electric oven for 10 hours at 80^oC. The autoclave was left into the oven after 6 hours to cool down at room temperature to ensure the complete chemical reaction.

6) To remove residual Na^+, the obtained precursor was washed several times with water. The residual was placed in an oven to dry at 80^o C for more than 8 hours.

7) The dried sample was then heat treated in a muffle furnace for 5 hours at 500^oC.

8) The obtained product was grinded by mortar pestle to get fine powder and then was placed in a vacuum desiccator.

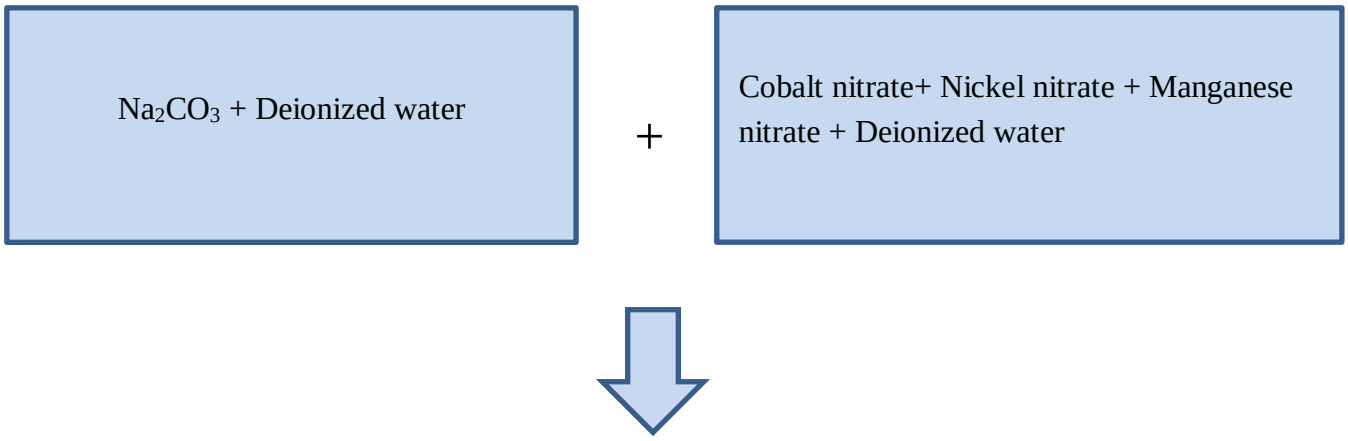

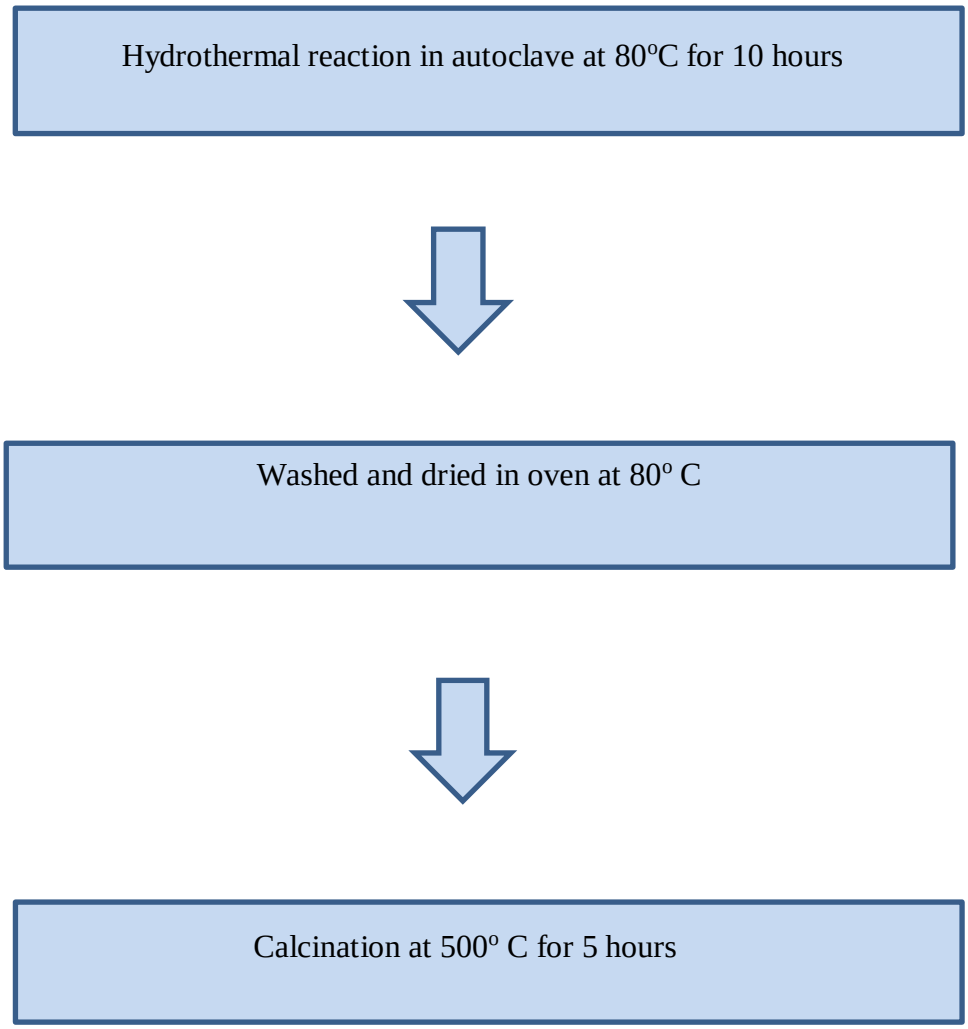

Figure 3.1 Synthesis of MNC

3.2 Synthesis of MNC-GNP

Instrument used during the process are:

- Teflon lined stainless steel autoclave
- Oven
- Magnetic stirrer
- Hotplate
- Beakers
- Petri dish
- Weighing balance

- Muffle furnace

Materials used for the synthesis of MNC-GNP are listed below

Materials	Purity level	Company name
Manganese nitrate tetrahydrate	**99**%	**Sigma Aldrich**
Copper nitrate hexahydrate	**99%**	**Sigma Aldrich**
Nickel nitrate hexahydrate	**98%**	**Merck Company**
Sodium carbonate	**98%**	**Thermo Fisher**
Graphene nanoplatelets	**95%**	**----------**
Deionized water	**99%**	**Sigma Aldrich**
Ethanol	**97%**	**Sigma Aldrich**

Table 3.2 materials to be used in synthesis of MNC-GNP

3.2.1 Process:

1) Hydrothermal method was used for the synthesis of MNC-GNP. A schematic route for synthesis of MNC is represented in Fig 2.2.

2)1M Nickel nitrate hexahydrate, 1M cobalt nitrate hexahydrate, 1M manganese nitrate tetra hydrate and 0.1g GNP were added in 10ml of deionized water under constant stirring.

3) In another beaker, an appropriate amount of sodium carbonate was added in 60ml of deionized water under constant stirring to ensure proper dissolution.

4) Then the Na_2CO_3 solution was poured into other metal nitrate solution drop wise under constant stirring.

5) Then this homogeneous solution was transferred into a Stainless steel autoclave and placed in an electric oven for 10 hours at 80^o C. The autoclave was left into the oven after 6 hours to cool down at room temperature to ensure the complete chemical reaction.

6) To remove residual Na^+, the obtained precursor was washed several times with water. The residual was placed in an oven to dry at 80° C for more than 8 hours.

7) The dried sample was then heat treated in a muffle furnace for 5 hours at 500°C.

8) The obtained product was grinded by mortar pestle to get fine powder and then was placed in a vacuum desiccator.

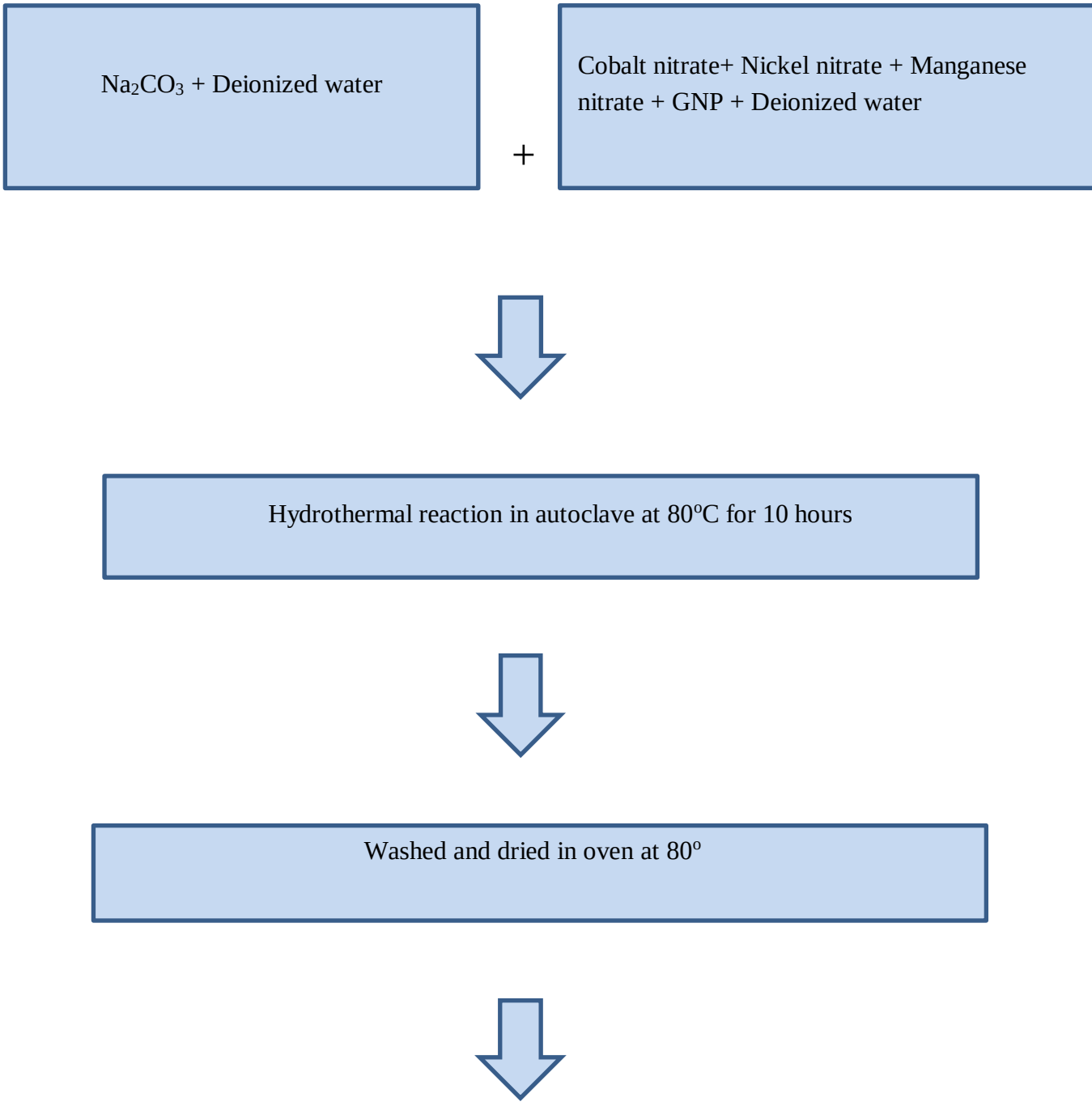

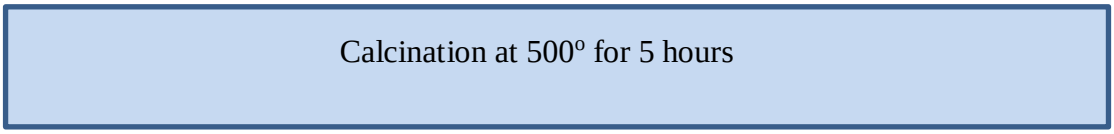

Figure 3.2 Synthesis of MNC-GNP

Summary

In this chapter, synthetic route used for the preparation of samples along with the chemicals are given.

Chapter 4

Characterization Techniques

4.1 X-ray diffraction (XRD)

In 1912, Max Von Laue won the noble prize on its work on X-rays diffracted by the solid crystals. It is a destructive technique that is used for the identification and quantification of crystal phases, the spacing between the lattice planes and their distance scale etc. In short, XRD provides information about the fingerprints of bragg's reflection of crystalline material.

The seven crystal systems are

- Cubic (isomeric)
- Tetragonal
- Triclinic
- Orthorhombic
- Hexagonal
- Monoclinic
- Trigonal

Samples of different natures such as organic, inorganic, polymers, metals and different composites can be analyzed. The sample of interest should be crystalline in nature. The wavelength of X-rays applied for analysis ranges from 10A to 2.5 nm. It consists of five main components,

- Radiation source
- Sample holder
- Component to limit wavelength range of received radiations
- Radiation transducer
- Signal processing and read out component

In most of the diffractometers, the X-ray source are placed along with the detectors at the same side of the sample the incident rays strike at some angle, reflected and onto the detector. Cathode ray tube contains a filament which is heated to generate electrons. Electric field is applied along with the direction of target to accelerate electrons towards target. characteristic X-rays are produced when these electrons strike the inner shells of the target material. Copper (Cu-Kα radiation= 1.5418Å) is the most commonly used target material for X-ray diffraction. Then this monochromatic X-ray beam is directed to fall on the sample. The angle is maintained by the unit called goniometer. Scintillation counter is the most commonly used detector which records the intensity of reflected X-rays obtained by constructive interference. The complete scan range of powder x-ray diffraction ranges from 5^{o} to 150^{o} [88].

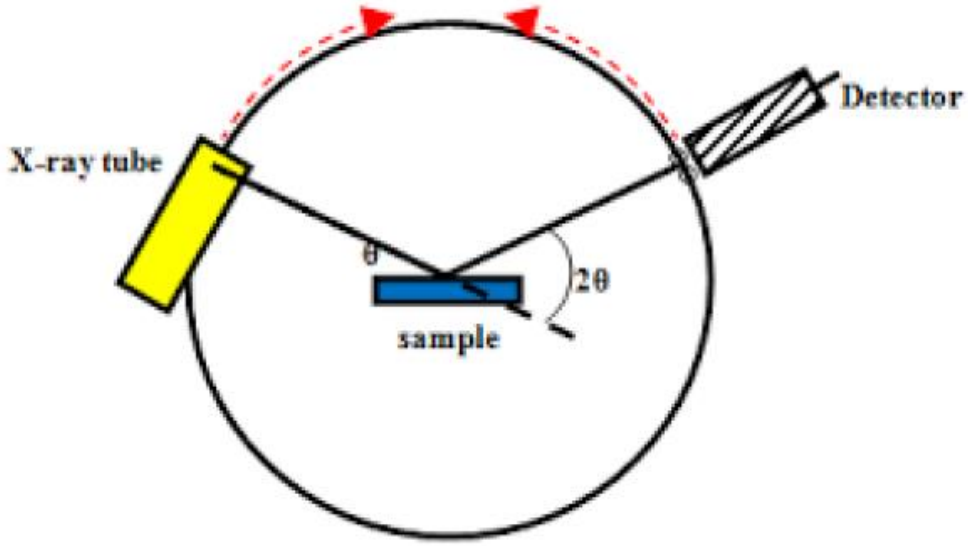

Figure 4.1 Components of XRD

Crystal is composed of layers and planes. When the X-ray light falls on the crystal, it gets dispersed by these layers and planes. If the wavelength of X-ray light matches with the planes of crystals, it is reflected in such a way that angle of incidence is equal to the angle of reflection. Interference occurs depending upon the spacing between the planes which results into the diffraction patterns [88].

In 1912, the relationship between scattering angles, d-spacing and wavelength of X-rays being used was given by W. H. Bragg and W. L. Bragg. It is stated as

$$n\lambda = 2d\sin\theta$$

Constructive interference takes place when bragg's law is satisfied. This technique tells us about different features of sample such as

- Sample purity
- Phase
- Crystallinity
- Lattice mismatch
- Dislocations
- Unit cell dimensions

4.2 Scanning Electron Microscope (SEM):

Scanning electron microscopy is a technique used for the investigation of morphology of materials, chemistry, crystallography and orientation of planes. Manfred Von Ardenne designed SEM for the first time in 1938. The sample to be analyzed by SEM should be conducting. A thin layered coating of gold or graphite is done on non-conducting samples so that analysis can be performed [89]. A high energy electron beam is bombarded on the material under analysis to produce 3D image with a resolution up to 1nm. Degree of magnification can be controlled by electromagnets. Surface of the material is focused by a fine beam of electrons. As a result electrons or photons are knocked out of the surface and directed towards detector. The output from the detector modulates the brightness of the cathode ray tube (CRT). For every point where electron beams are focused and interact, it is plotted on consequent points on CRT. As a result, 3D image of the material is produced.

The interaction of electron beam with matter generates secondary electrons (SE), backscattering electrons (BSE) and X-rays. Commonly used SEM mode is through secondary electrons. These electrons are emitted near sample surface which results into a pronounced and clear image. Back scattering electrons are produced by elastic scattering of incident electrons. They emerge from deeper locations as compared to

secondary electrons so have low magnification comparatively. Characteristic X-rays are produced when an inner shell electron is knocked off from its shell.

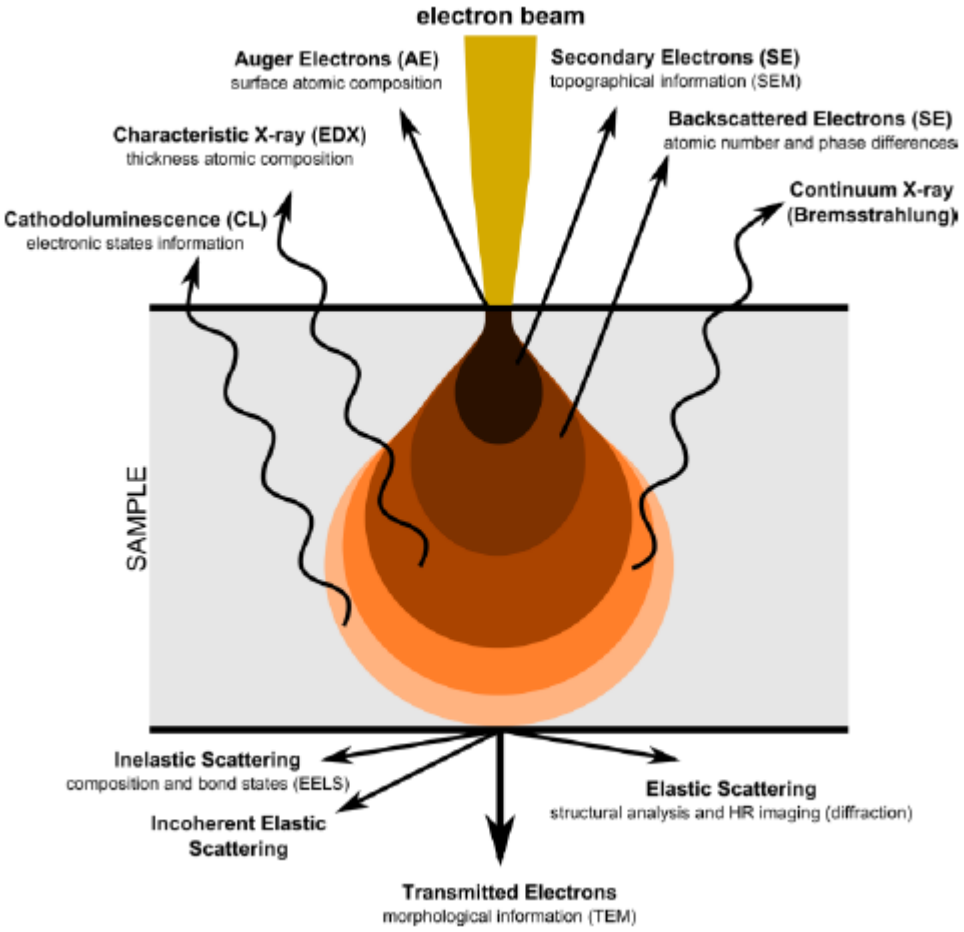

Figure 4.2 Possible emissions in SEM operation

4.2.1 Construction of SEM

SEM consists of following components;

- Electron Gun
- Electromagnetic lens
- Object chamber
- Secondary electron detector
- Display unit

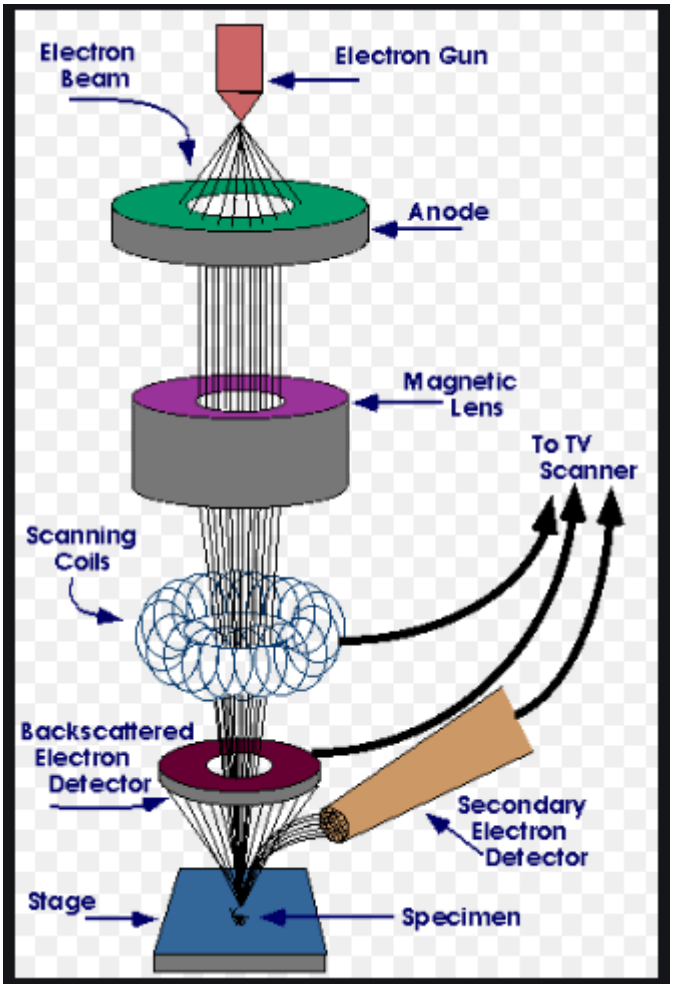

Figure 4.3 Schematic of SEM

4.2.2 Working of SEM

Upon heating, electron gun emits a stream of monochromatic electrons which are focused by electromagnetic lenses. Diameter and current of the beam is controlled by the condenser lens by optimizing the number of beams. Coherency of the beam is maintained by second lens. The scanning coils used to scan the beam in a grid fashion. Lastly, the electron beam is focused on sample with the help of objective lens. Sample holder is used to insert sample in the vacuum chamber. For better area analysis, the holder can be moved in X and Y direction and rotated, tilted and moved in Z direction for better resolution. At the rear of sample holder, secondary electron detector is located. Surface structure of material affects the velocity and angle of secondary

electrons. When the electrons are focused on the detector, electronic signals are produced. These electronic signals are amplified and transformed into digital signals. For further processing, these digital signals are observed on display unit. [89]

Various signals are produced as a result of interaction between electron beam and the surface of material. Each different signal provides us with the different information about the sample under study. BSE and SE are commonly used for imaging [90].

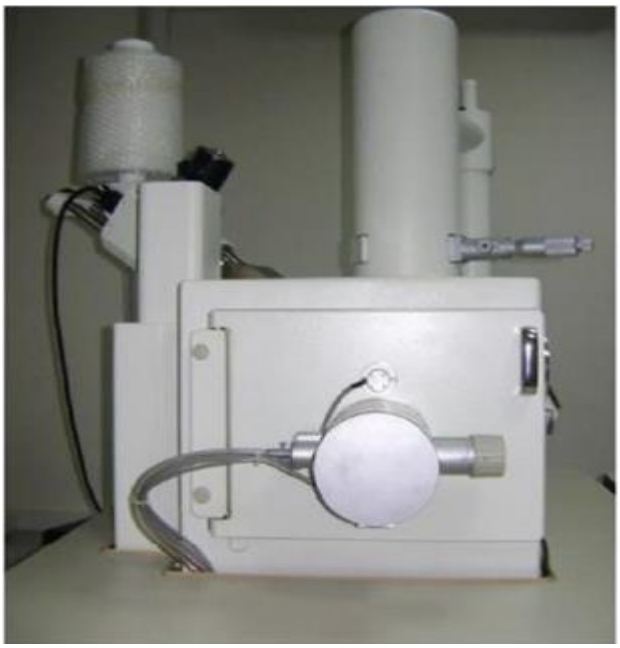

Figure 4.4 JOEL JSM-6490LA present at SCME

4.3 BET Surface area analysis

Material is analyzed for the determination of porosity and surface area of the material through BET analysis. Non corrosive gases like N_2 are used in BET which is adsorbed or desorbed on the surface of material. Sample is dried at high temperature with the purging of N_2 gas. The surface area and porosity are determined by the amount of adsorbed N_2 gas on the surface of material. Volumetric or continuous flow process is used to investigate the amount of gas adsorbed on the surface. Weak Van der Waal's forces exist between N_2 gas and sample surface and these interactions are performed at liquid nitrogen temperature. BET isotherm equation is given as

$$\frac{1}{V_a\left[\frac{P_0}{P}-1\right]} = \frac{C-1}{V_m\,C} \times \frac{P}{P_0} + \frac{1}{V_m\,C}$$

This equation is used in BET multipoint measurement. Specific pore surface area can be calculated by using values V_m and mass of material used. BET analysis technique is used to calculate surface area and porosity which are very important characteristics of the sample. The equipment consists of several parts including sample preparation device, sample tube, vacuum pump, N_2 transfer system, computer hardware and software. Sample is dried at the high temperatures with the purging of non corrosive gases like N_2 then the specific surface area and the pore size is calculated by the amount of gas adsorbed. Sample preparation is one of the most crucial steps of the analysis. Firstly the purification of the sample is done by degassing in vacuum conditions for a particular amount of time in the sample preparation device so that all the contaminants like gas molecules and water vapours can be removed. Then the sample test tube was placed in the surface area, and porosity analysis which relates to the computing system and amount of adsorbing gases is calculated, related to the surface area and total pore volume [91][92].

4.3.1 Sample preparation:

Firstly, degassing is performed in order to purify sample from different atmospheric contaminants like water vapors, air etc at elevated temperature. Vacuum conditions are required for degassing.

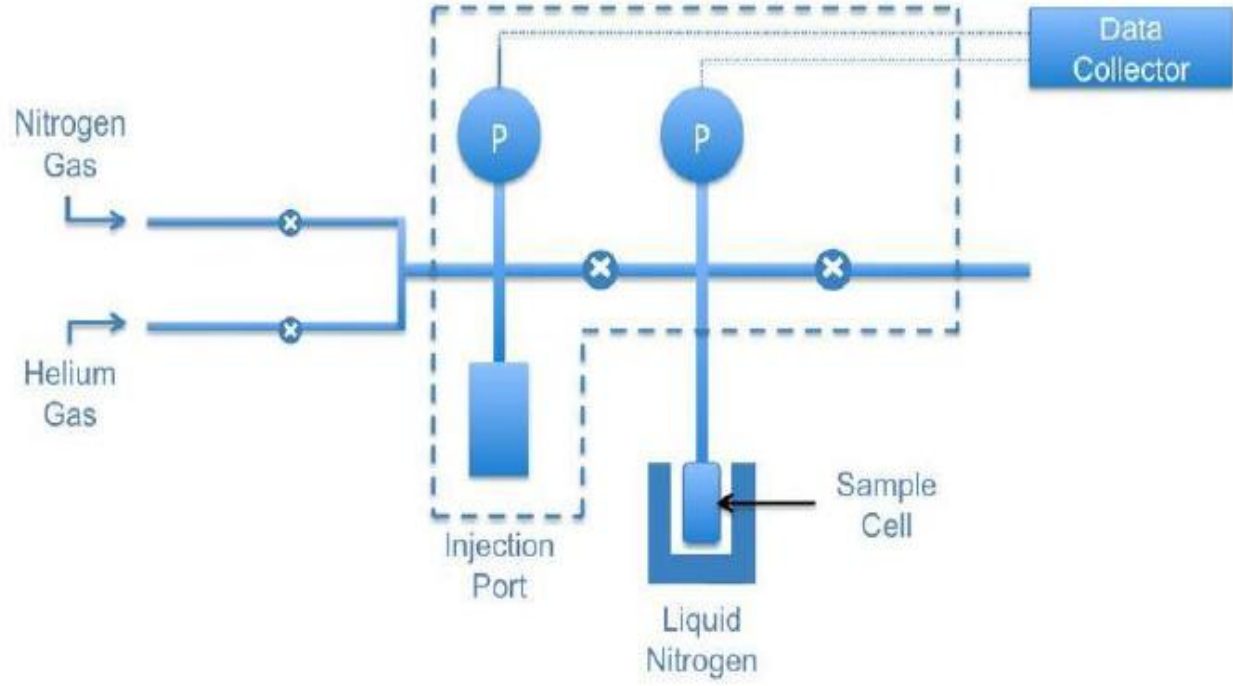

4.3.2 Instrumentation:

Instrumentation consists of following components

- Sample tube
- Reference tube
- Monometer
- Gaseous pressure inlet
- Inert gas inlet and vacuum system
- Temperature controlled system from high temperature system low temperature

Figure 4.5 Gemini® VII 2390 Micro porosity analyzer

4.4 Electrochemical analysis

Electrochemical analysis is a method in which analyte is analyzed in an electrochemical cell by the measurements of current and voltage.

Three basic types of electro-analytical methods are

1) Potentiometry:
   Potential of the electrode is measured in potentiometry.
2) Coulometry:
   In coulometry, current is measured against time i.e. current is measured as a function of time.
3) Voltammetry:
   In voltammetry, current is measured as a function of time.

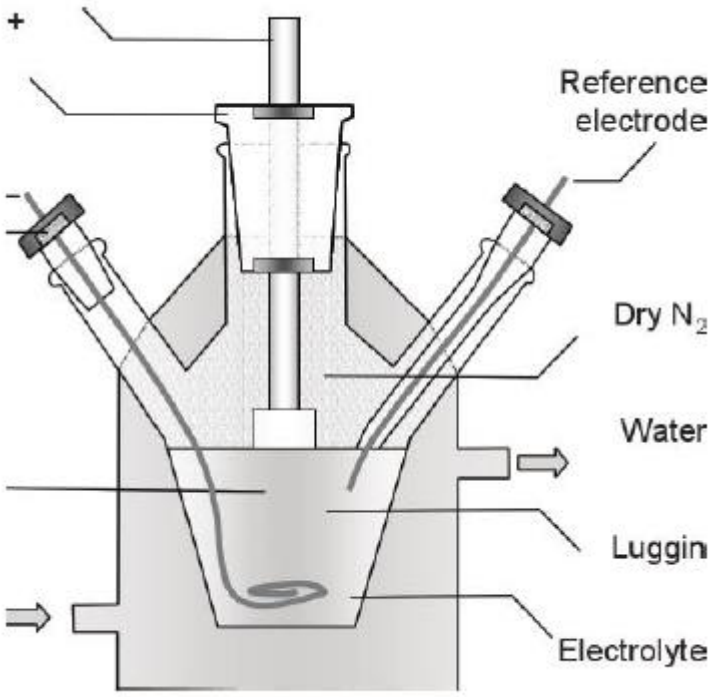

Figure 4.6 Electrochemical workstation electrodes assembly

Generally, electrochemical electrode assembly consists of three electrodes: Reference electrode, counter electrode and working electrode

Reference electrode is the standard electrode used to measure the potential of working electrode relative to reference electrode. Standard hydrogen electrode (SHE) and Ag/AgCl are used as reference electrode. Reference electrode has fixed potential value.

Counter electrode is also called auxiliary electrode, it is the current conducting electrode that completes the electrical circuit in an electrochemical cell. Generally platinum wire and carbon based electrodes are used as counter electrode. Electrode should satisfy certain conditions to act as counter electrode such as:

- Electrode material should be insoluble in electrolyte of electrochemical cell.
- Counter electrode should not disturb the working electrode in a way that generated products must not react with working electrode.
- Counter electrode should have area larger than working electrode.

Working electrode is inert electrochemically in the analysis window. Glassy carbon, nickel foam are generally used.

Electrochemical workstation can be used for many applications

- Battery testing
- Capacitors and super capacitor testing
- Corrosion testing
- Fuel cell and biofuel cell
- Photovoltaics and sensors

Supercapacitor testing involves

- Cyclic voltammetry (CV)
- Galvanic charge discharge (GCD)
- Electrochemical Impedance spectroscopy (EIS)

Figure 4.7 Electrochemical workstation in SCME

4.5 Cyclic voltammetry

Electrochemical behavior of a material is measured by CV analysis on a laboratory scale. Oxidation-Reduction reaction are analyzed through CV that occur at the interface of the electrolyte/electrode. CV system comprises of three electrodes. In CV, a potential is charged on reference electrode and working electrode and resulting output current responses are recorded between working and counter electrode. CV curve is resulting current (I) vs potential (V) of working electrode. Potential is applied between WE and RE. Platinum is the commonly used counter electrode. Electrolyte should have high conductivity. The basic function of electrolyte is to provide ion. Different responces are being observed by different kind of materials. EDLC gives rectangular curves whereas oxidation reduction humps are given by pseudocapacitor during forward and reverse scan.

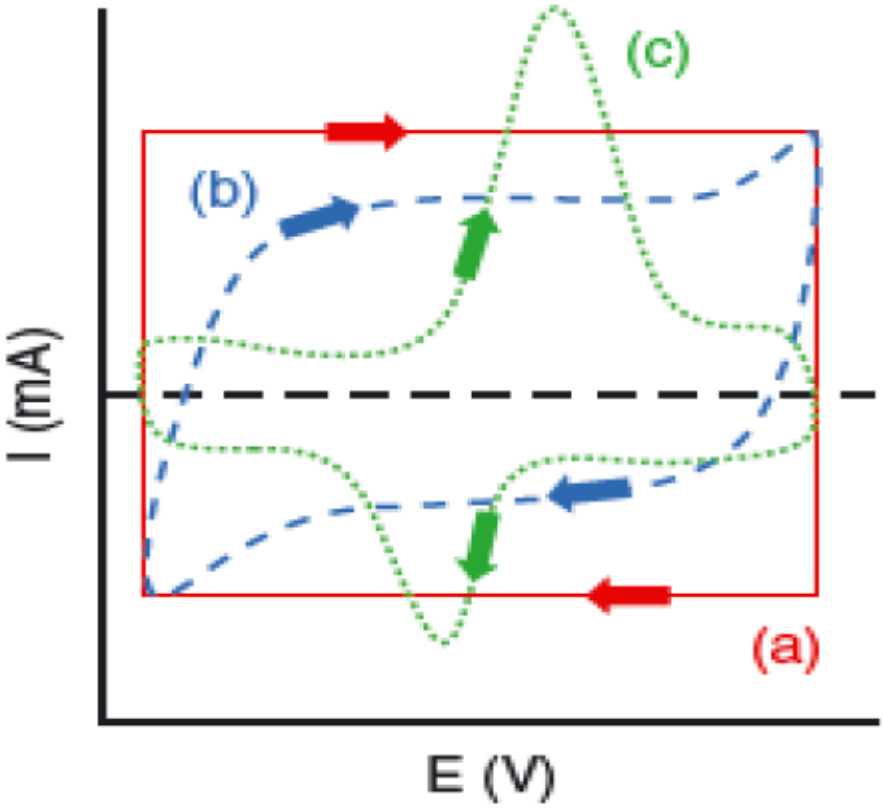

Figure 4.8 CV curves for (a) Ideal case (b) EDLC (c) pseudocapacitor [93]

4.6 Galvanic charge discharge (GCD)

Charging and discharging of batteries and supercapacitors is tested through GCD. One charge and discharge of material equals to one cycle. GCD measures the potential with time at constant current. The main working concept of GCD is that impulse is applied on working electrode which generates the potential. Then the measurements are done on potential as a function of time.

EDLC and supercapacitor show different curves in GCD similar to CV. EDLC shows linear curve while pseudocapacitors show a non linear curve. The difference in the behavior is due to different charge storage mechanism. In EDLC, charge is stored physically while in pseudocapacitors, charge is stored through faradaic reactions. The main difference between GCD and cyclic voltammetry lies in the current which is controlled in GCD and measurements on voltage are done. GCD is also called chronopotentiometry, and it is one of the most extensively used technique in laboratories and industries for testing of electrochemical behavior of a material.

It gives insight of the following parameters

- Resistance
- Capacitance
- Stability

In a V (t) profile of a supercapacitor, V (t) does not vary linearly.

So capacitance is given by

$$\mathbf{C = I\Delta t\Delta V}$$

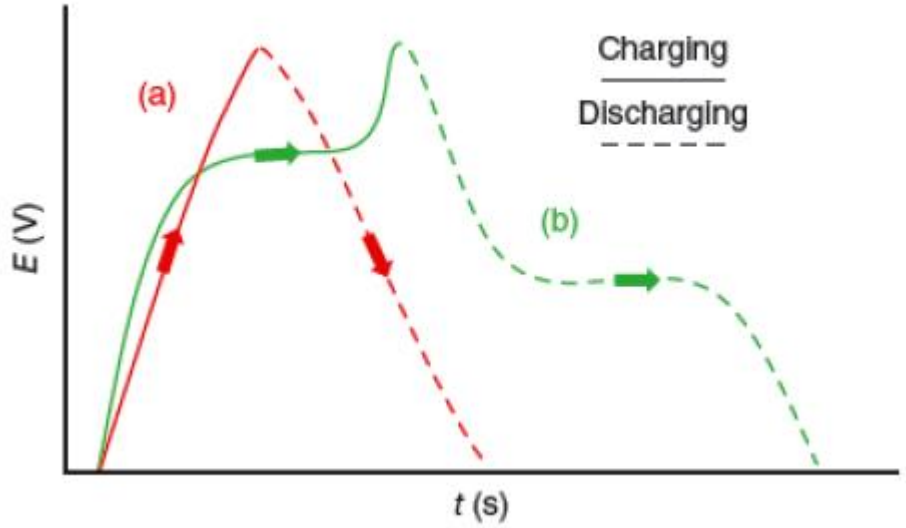

Figure 4.9 GCD curves for (a) EDLC (b) pseudocapacitor [93]

4.7 Cyclic stability

One of the most important parameter to verify the electrochemical behavior of a material is cyclic stability which is tested by multiple charge and discharge cycles. Normally 500 to 10000 cycles are conducted in lab to examine capacitance retention of material.

4.8 Electrochemical impedance spectroscopy:

Electrochemical impedance spectroscopy has been extensively use in sensing, corrosion, fuel, capacitor and resistance studies. Impedance analysis of material is done by using this technique.it is a sensitive technique which provides information about interface electrochemical reaction [94-96]

4.8.1 Working principal:

When the alternating current signals are applied, the responses of the analyte are recorded. EIS is a sensitive techniques performed at different frequencies to detect the analytes. The only disadvantage of EIS is its low selectivity of input parameters [97, 98]. The curve of EIS consists of two parts, a semicircle and a real axis. The real axis

should be vertical and semicircle should be smaller for an ideal case for a capacitive material. In EIS, the shape of curvature depends upon the nature of material. Nyqusit plot is analyzed for determination of value of resistance. An appropriate circuit is selected to perform the z-fitting to analyze the impedance of the system.

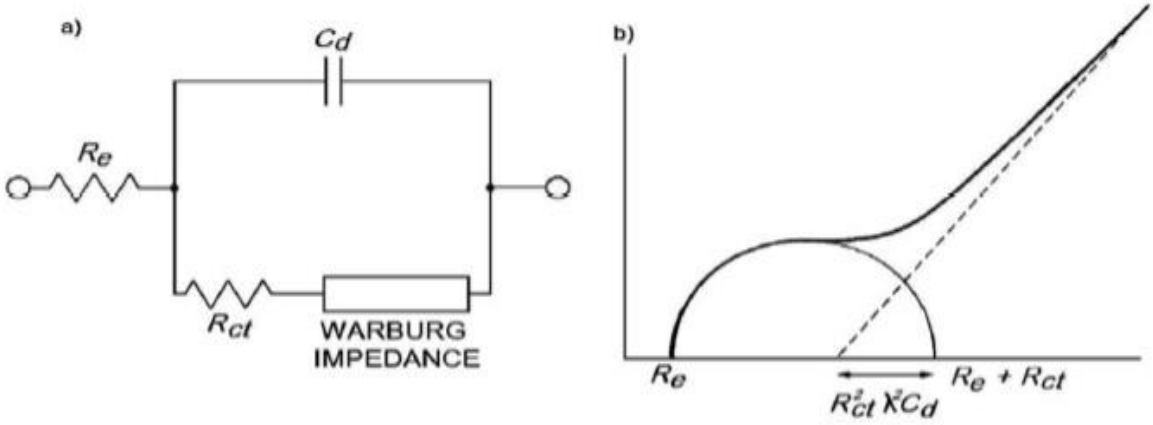

Figure 4.10 EIS (a) Equivalent circuit Diagram (b) Nyquist plot

Here;

Re is the solution resistance which is the series resistance at working electrode/electrolyte interface

Rct is the charge transfer resistance or polarization resistance

Cd is the double layer capacitance which is the interface capacitance between electrode and electrolyte and wanburg impedance which depends upon the diffusion of reactant.

Summary

In this chapter, different characterization techniques used for the analysis of material are discussed. Basic concepts along with the instrumentation and working of every technique is given.

Chapter 5

Results and Discussion

Literature review about the supercapacitive performance of the supercapacitor has revealed that the metal oxide based electrode material have high pseudocapacitance but limitations like excessive loss of capacitance over prolong charge discharge cycles and volume induces structural variation are still big challenges. Short life cycle and excessive capacity loss are observed which affect the electrochemical characteristics of the TMOs based electrode materials. On the other hand carbon based material have good mechanical strength, electrical properties and good life cyclability but are limited by low EDLCs performance. Consequently, combining metal oxides with different carbonaceous nanostructures based electrode systems are expected to give good results due to synergistic effect.

So this research work is designed to exploit the pseudocapacitance of ternary transition metal oxides and good durability of graphene nanoplatelets to cope with the challenges faced in the field of supercapacitors. In this research composite of ternary oxides of manganese, nickel and cobalt with graphene nanoplatelets and copper are prepared via hydrothermal approach. This chapter gives the insight about the results obtained from different characterization techniques and electrochemical testing performed in order to check the electrochemical performance of the material to be used as an electrode material for supercapacitor.

5.1. Morphological analysis of nanostructure

SEM was performed for the structural analysis of the synthesized material. Each of the synthesized metal oxide composite is dissolved in DI water and ultrasonication is done for 2 hours. Then a drop of dispersion is put on a cleaned glass slide and dried. Gold coating is done on the sample to make it conductive by using ion sputtering system. Then SEM is performed on the samples.

5.1.1 MNC

Fig. 5.1(a) shows the image of MNC at low resolution. It revealed that our synthesized MNC consists of plant like dendrites growing randomly. Fig 5.1 (b) and (c) gives the high resolution of MNC with high depth of focus to visualize the small agglomerated particles of average size of 90.75nm dispersed along the dendritic plant like structure. These small particles were then agglomerate to give dendritic outgrowths.

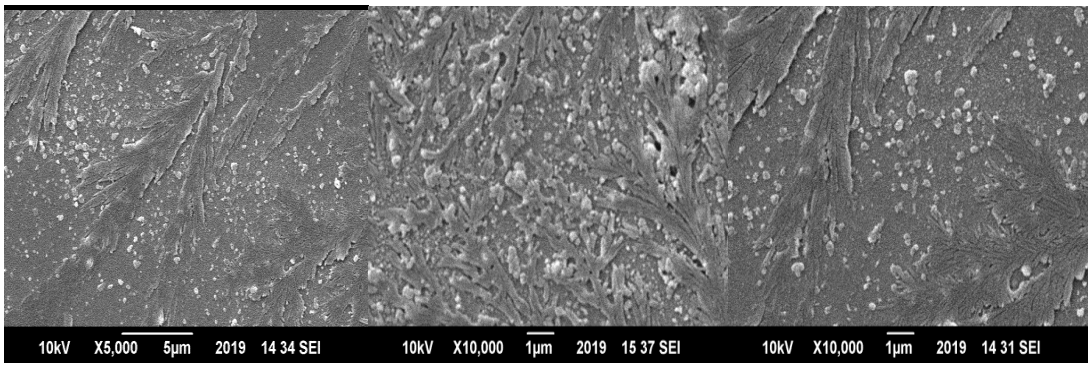

Fig 5.1 (a) SEM image for MNC at low resolution (b) and (c) SEM image at high resolution

5.1.2 MNC-GNP Composite

Fig. 5.2 reveals the distinct hierarchical dendrites structure of MNC ternary oxide with graphene nanoplatelets composite. Unique dendrite morphology of ternary MNC oxide with GNPs offer enhanced electrochemical properties for the supercapacitor.

The self-assembly and aggregation of metal nanoparticles is facilitated by the addition of graphene nanoplatelets, leading to the formation of plant like dendritic structures. Graphene nanoplatelets improve the electrochemical properties of composite material as well as it also facilitates fast transportation of electrons during electrochemical reaction. Though the 3D hierarchical dendrites still appeared in Fig. 5.1 but they reveal extremely low in density and outgrowths but this sample consists of a number of branches densely packed together with affordable high porosity which favors the facile access of electrolyte ions which may contribute to the optimization of electrochemical performance.

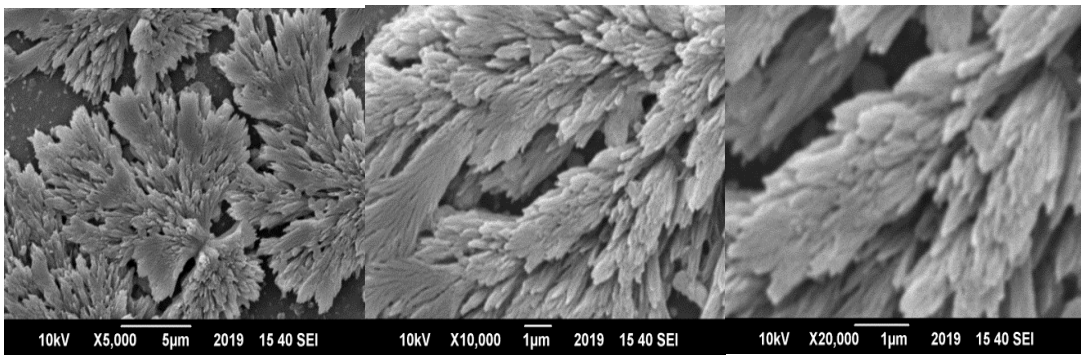

Fig. 5.2 SEM images of MNC-GNP at different resolutions (a) X=5000 (b) X=10000 (c) X=20000

5.2 Phase structural analysis

5.2.1 XRD of MNC

Structural and compositional analysis of the synthesized MNC was done through XRD. The results from XRD represent the formation of cubic structure in a complete agreement with JCPDS card no. 02-0925. There are no peaks of any impurities were seen in XRD. The maximum X-ray diffraction observed along the crystal planes (111) assigned at diffraction positions of $2\theta = 16^{o}$. The other peaks are observed at 30^{o}, 32^{o}, 34^{o}, 37^{o}, 42^{o}, 44^{o}, 46^{o}, 48^{o}, 54^{o}, 59^{o}, 63^{o}, 69^{o} and 76^{o} which correspond to planes (131), (220), (311), (222), (220), (400), (421), (113), (422), (511), (440), (243) and (533).

Average crystallite size calculated by observed XRD peaks was 8.66 nm. The Scherrer formula is given as

$$D=0.9\lambda/(\beta\cos\theta)$$

5.2.2 XRD of MNC-GNP

Structural and compositional analysis of the synthesized MNC-GNP was done through XRD. The results from XRD represent the formation of cubic structure in a complete agreement with JCPDS card no.02-0925. There are no peaks of any impurities were seen in XRD. The maximum X-ray diffraction observed along the crystal planes (111) assigned at diffraction positions of $2\theta = 16^{o}$. The other peaks are

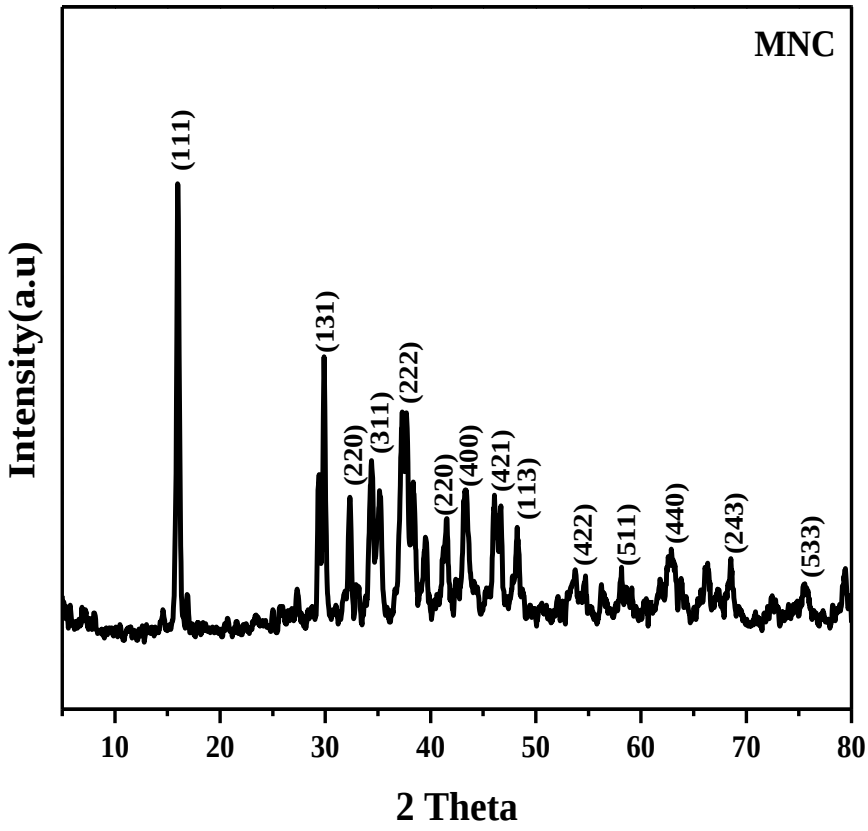

Fig 5.3 XRD analysis of MNC

observed at 30^o , 32^o , 34^o , 37^o , 42^o , 44^o , 46^o , 48^o , 54^o , 59^o , 63^o , 69^o and 76^o which correspond to planes (131), (220), (311), (222), (220), (400), (421), (113), (422), (511), (440), (243) and (533) . Average crystallite size calculated by observed XRD peaks was 9.30 nm. The Scherrer formula is given as

$$D=0.9\lambda/(\beta\cos\theta)$$

5.2.3 Combined XRD for comparison

Fig 5.6 shows the comparison of XRD of MNC and MNC-GNP. Average crystallite size is ranges between 8.66 to 9.30 nm by the addition of Graphene nanoplatelets. Moreover, a peak was observed at 26.4^o in second sample which depicts the presence

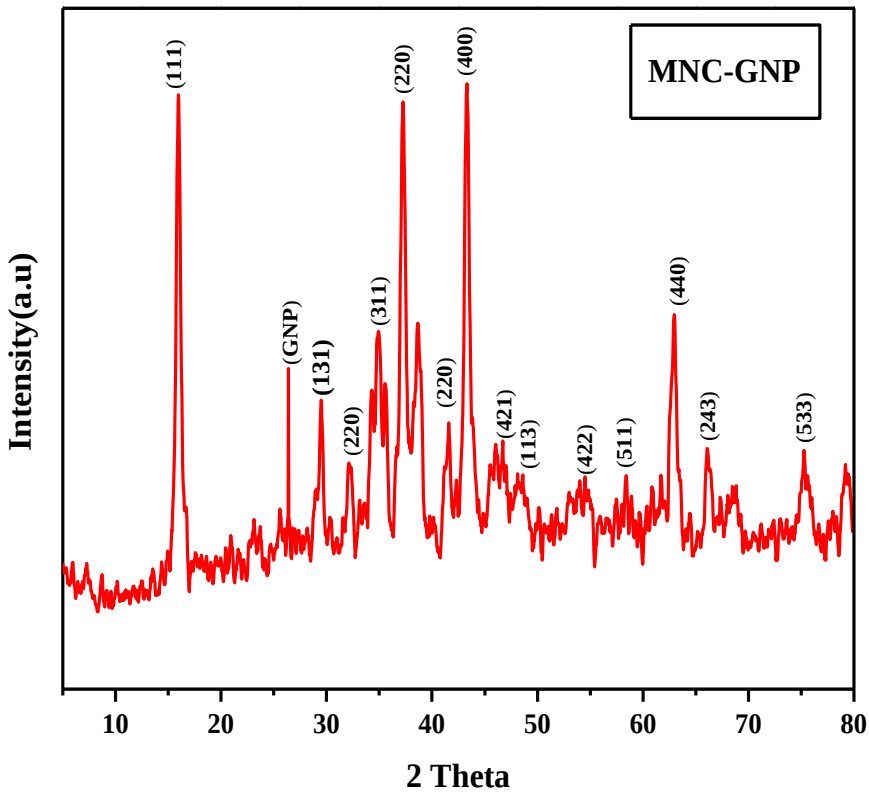

Fig 5.4 XRD analysis of MNC-GNP

of GNPs. The peak of graphene nanoplatelets becomes sharp by the increase in concentration of GNPs. Hence synthesis of composite of MNC-GNP is confirmed by XRD.

5.3 Electrochemical studies of MNC and MNC-GNP

The electrochemical analysis of MNC and MNC-GNP were performed in a three electrode system. The electrolyte used in this process was 2M solution of potassium hydroxide. A homogeneous slurry was prepared by mixing active material MNC and MNC-GNP powders with carbon black as conducting agent and polyvinylidine diflouride as a binder (Mass ratio 85:10:5)to be used as working electrode.

The substrate Nickel foam was used as an electrode material. It was washed with 6M HCl in an ultrasonication bath for 15 minutes to remove the layer of NiO on surface. Then washing with water and absolute ethanol is done. Washed Nickel foam was then

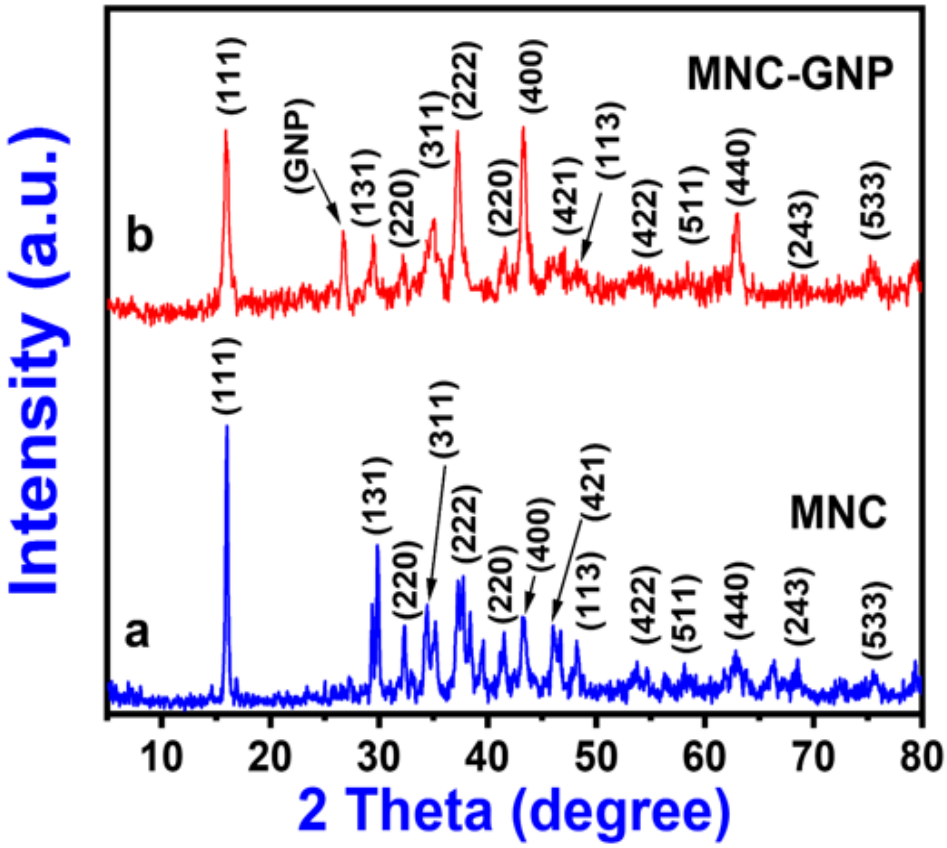

Fig 5.5 Comparison of XRD

dried for 4 hours at 70°C. It was then coated with homogeneous slurry and then pressed at 10Mpa. It is then dried under vacuum at 70° C for 18 hours. The mass of active material on the electrode ranges between 1.3-1.8mg. Three electrode system consisting of working electrode, platinum as counter electrode and Ag/AgCl as reference electrode was used and 6M KOH was used as electrolyte at room temperature.

Cyclic voltammetry (CV), galvanic charge discharge (GCD) and Electrochemical Impedance Spectroscopy (EIS) were conducted to characterize the electrochemical behavior of MNC and MNC-GNP electrodes. The nickel foam of 1×1 cm was connected with a wire by soldering and dipped in the electrolyte for electrochemical measurements.

5.4 Cyclic voltammetry (CV)

It was carried out to visualize the capacitive response of MNC and MNC-GNP at different scan rates.

5.4.1 MNC

To evaluate potential application in electrochemical supercapacitor, prepared composite was applied as active material in a three electrode configuration. Figure 5.6 shows the CV curves of MNC are obtained at the scan rate of 2 mVs^{-1}, 5mVs^{-1}, 10 mVs^{-1},50 mVs^{-1}, 100 mVs^{-1} , 200 mVs^{-1} and 500mVs^{-1}in 2M KOH electrolyte. Potential range was kept 0-0.6 during CV analysis. The shape of CV curves deviate from ideal rectangle, non-rectangular graph of cyclic voltagramm for MNC showed the pseudocapacitive nature of the sample. The value of current in response to the applied potential difference increases with the scan rate. Specific capacitance was calculated at different scan rates by

$$Cs = \frac{\int idV}{(Vs * m * \Delta V)}$$

Where Cs = Specific capacitance

$\int idV$ = Integrated scan rate

Vs = scan rate

m = active mass

ΔV = Operating potential window

MNC nanodendrites exhibited capacitance of 1455.5 Fg^{-1} at 2 mVs^{-1} , 662 Fg^{-1} at 5mVs^{-1} , 372 Fg^{-1} at 10mVs^{-1} , 118.4 Fg^{-1} at 50mVs^{-1}, 93.3 Fg^{-1} at 100mVs^{-1} , 81.1 Fg^{-1} at 200 mVs^{-1} and 46.2 Fg^{-1} at 500mVs^{-1}.

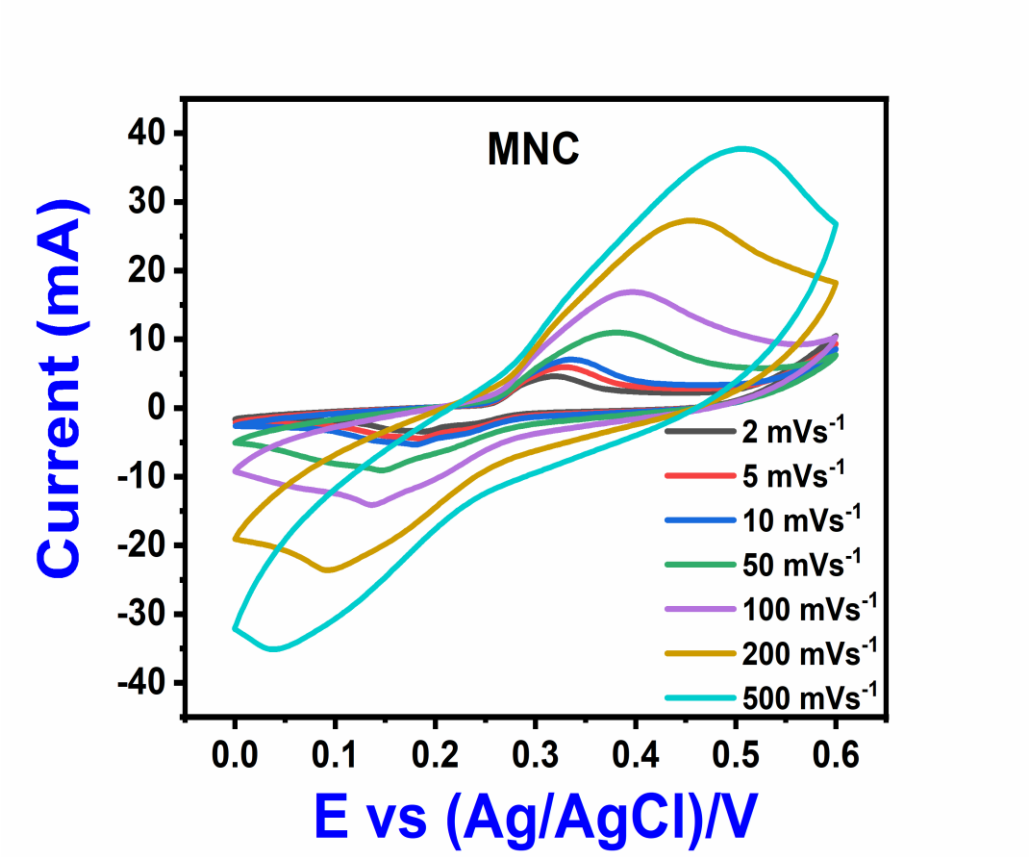

Fig 5.6 CV curves for MNC

5.4.2 MNC-GNP

Fig 5.8 shows the CV curves of MNC-GNP at the scan rate of 2 mVs^{-1}, 5mVs^{-1}, 10 mVs^{-1},50 mVs^{-1}, 100 mVs^{-1} ,200 mVs^{-1} and 500 mVs^{-1}. Potential range was kept 0-0.6 during CV analysis. The non-rectangular graph of cyclic voltagramm for MNC showed the pseudocapacitive nature of the sample. The value of current in response to the applied potential difference increases with the scan rate. Specific capacitance was calculated at different scan rates as

$$Cs = \frac{\int idV}{(Vs * m * \Delta V)}$$

Where Cs = Specific capacitance

$\int idV$ = Integrated scan rate

Vs = scan rate

m = active mass

ΔV = Operating potential window

MNC-GNP nanodendrites exhibited capacitance of 1816 Fg^{-1} at 2 mVs^{-1}, 1061 at 5 mVs^{-1} , 304.44 Fg^{-1} at 10 mVs^{-1} ,151.31 Fg^{-1} at 50 mVs^{-1} ,160.07 Fg^{-1} at 100 mVs^{-1} ,197 Fg^{-1} at 200 mVs^{-1} and 201.18 Fg^{-1} at 500 mVs^{-1}. Highest capacitance of 1816 Fg^{-1} is observed at scan rate 2 mVs^{-1} as it has the highest integrated area. High capacitance in MNC-GNP composite can be credited to the synergistic effect produced by metal oxides and graphene nanoplatelets. Addition of graphene nanoplatelets, though in a small amount, has affected the performance of the supercapacitor in a positive way. Faradaic process triggered by the addition of graphene nanoplatelets resulted into pseudocapacitive behavior providing highly conductive scaffold.

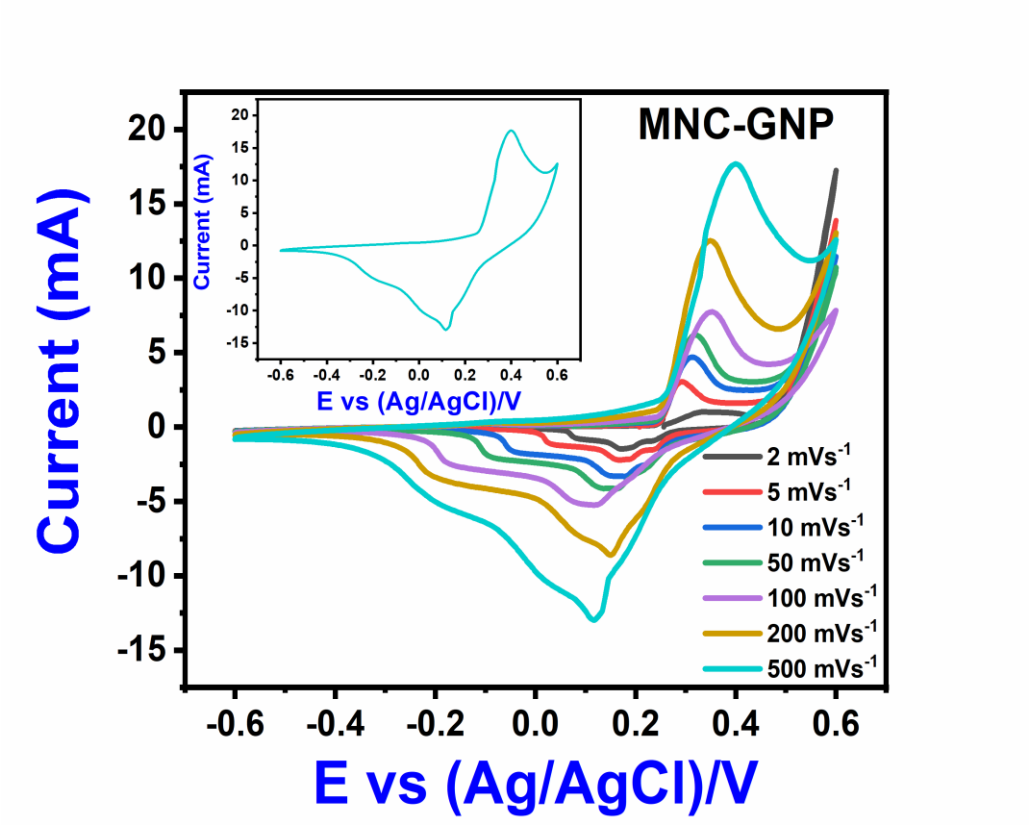

Fig 5.7 CV curves for MNC-GNP

Current density	C_s for MNC	C_s for MNC-GNP
2 mVs^{-1}	1455.5 Fg^{-1}	1816 Fg^{-1}
5 mVs^{-1}	662 Fg^{-1}	1061 Fg^{-1}
10 mVs^{-1}	372 Fg^{-1}	304.44 Fg^{-1}
50 mVs^{-1}	118.4 Fg^{-1}	151.31 Fg^{-1}
== 100 mVs^{-1}	93.3 Fg^{-1}	160.07 Fg^{-1}
200 mVs^{-1}	81.1 Fg^{-1}	197 Fg^{-1}
500 mVs^{-1}	46.2 Fg^{-1}	201.18 Fg^{-1}

Table 3. Specific capacitance for MNC and MNC-GNP at different current densities

5.5 Galvanostatic charge discharge (GCD)

Charge storage abilities of material are studies through galvanostatic charge discharge technique. GCD was used to observe the time required by the material to charge and then sustain the charge over a specific period of time.

5.5.1 MNC

GCD was performed for further studying of capacitive behavior of MNC after visualizing the capacitive behavior of the sample through cyclic voltammetry. Fig 5.9 shows GCD curves for MNC at 1 Ag^{-1}, 2Ag^{-1}, 3Ag^{-1}, 4Ag^{-1} and 5Ag^{-1} with operating window of 0-0.4. Maximum charge sustaining time was observed at a current density of 1Ag^{-1}. Non-linear response of the material shows faradaic behavior which depicts that the faradaic reactions occur and oxidation-reduction reactions are involved in charge storage mechanism.

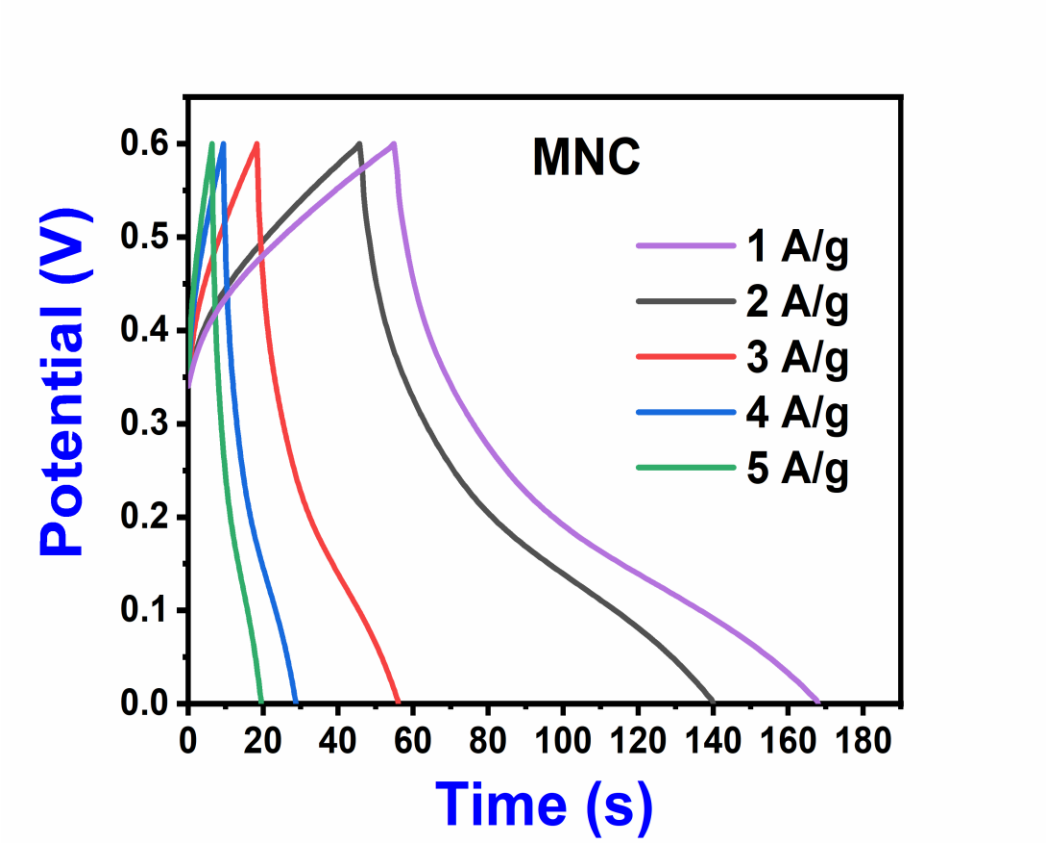

Fig 5.8 GCD graph for MNC

5.5.2 MNC-GNP

GCD was performed for further studying of capacitive behavior of MNC-GNP after visualizing the capacitive behavior of the sample through cyclic voltammetry. Fig 5.10 shows GCD curves for MNC at 1 Ag^{-1}, $2Ag^{-1}$, $3Ag^{-1}$, $4Ag^{-1}$ and $5Ag^{-1}$ with operating window of 0-0.4. Maximum charge sustaining time was 540s observed at a current density of $1Ag^{-1}$. Non linear response of the material shows faradaic behavior which depicts that the faradaic reactions occur and oxidation-reduction reactions are involved in charge storage mechanism.

GCD results have shown that MNC-GNP composite possess higher charge discharge time which is 540s as compared to its counterpart which is 169s at 1 A/g. It can be related to the synergistic affect produced by the combination of ternary metal oxides and carbon material. Presence of GNPs triggered the faradaic process resulting into higher conductivity.

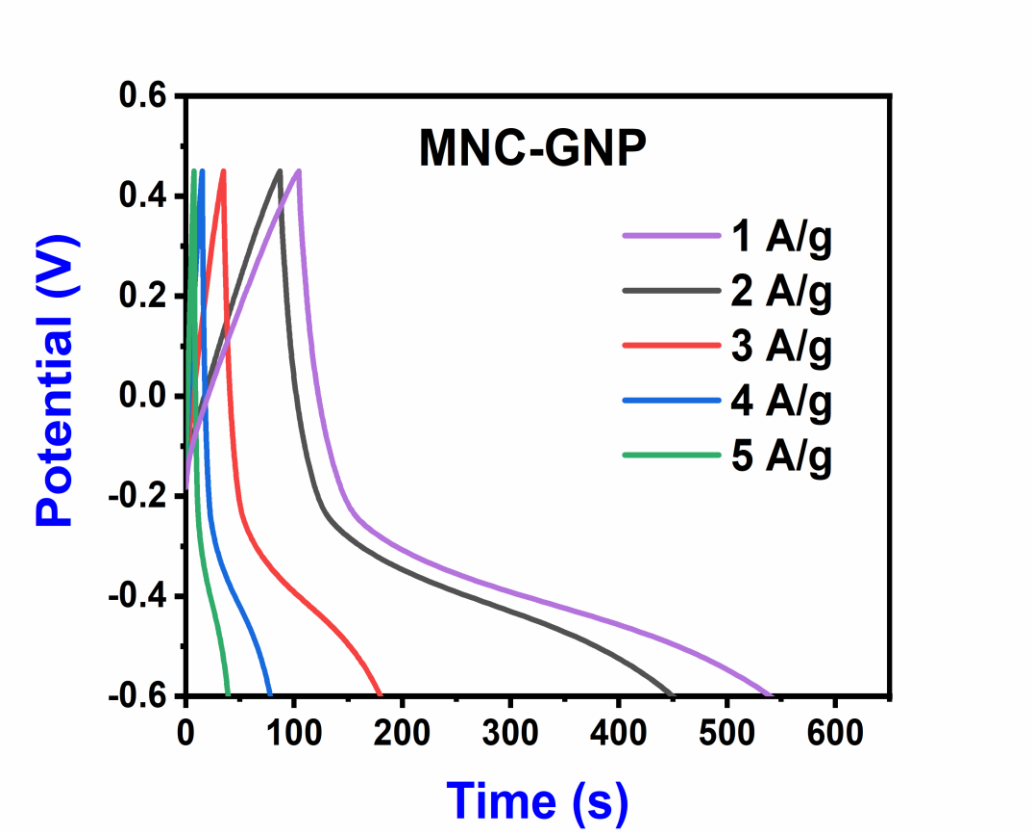

Fig 5.9 GCD graph for MNC-GNP

5.6 Charge stability

Charge stability is an important factor to check the feasibility of electrode material for supercapacitor for practical use. In order to check time for sustaining charge i.e. charge stability of MNC-GNP, GCD technique was performed. MNC-GNP composite exhibited good cyclic performance 99.5% of capacitance over 1000 cycles at 2 A/g.

MNC-GNP composite have shown enhanced supercapacitive behavior resulted into higher capacitance, enhanced cyclic stability, good capacitive retention and high energy density. These enhanced characteristics may be resulted due to unique

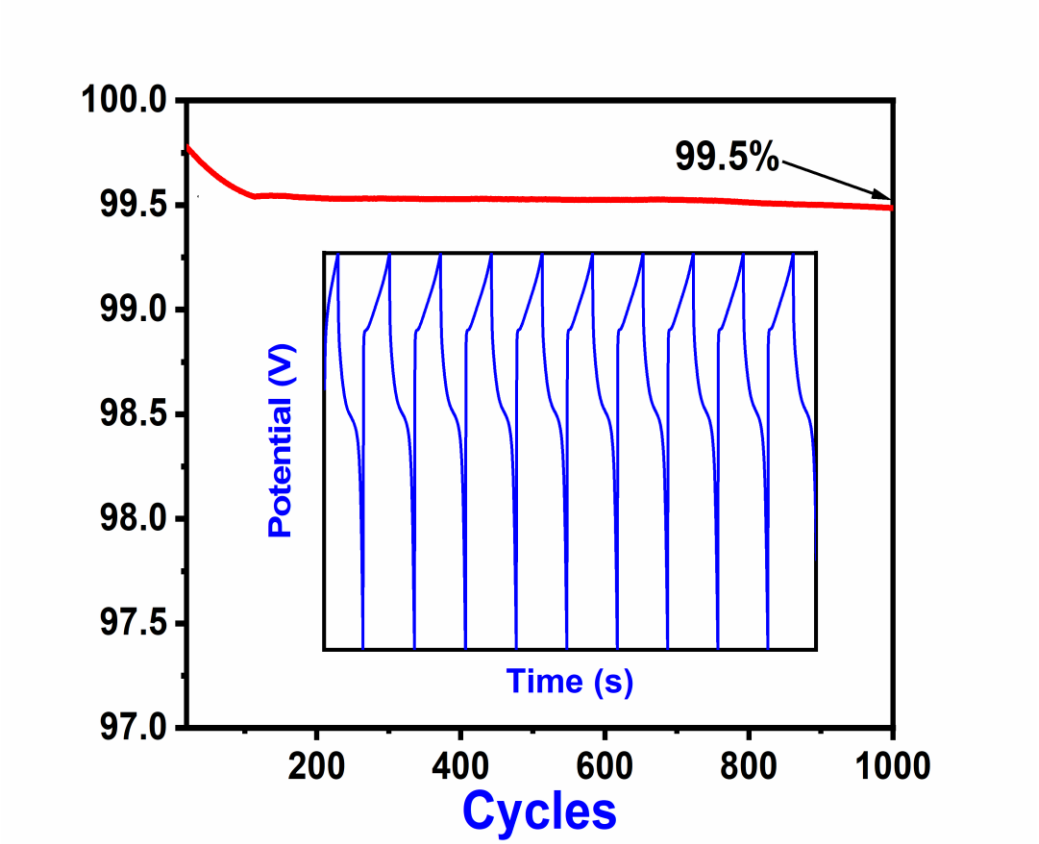

Fig 5.10 Cyclic performance

composition, reaction conditions and synergistic effect of ternary metal oxides with graphene nanoplatelets. Thus high surface area of GNP composite and reversible faradaic reactions exhibited high faradaic capacitance. High surface area provides electrolyte ions and electrons with higher penetration and transportation rate through pores which resulted into the better electrochemical performance. For super capacitor application, prepared composite of MNC-GNP proves to be a good electrode material

Summary

In this chapter, results of all the techniques that were used for the analysis of synthesized material are stated along with the discussions. The information on structural characteristics were obtained through XRD. SEM was done to know the morphology of particles. Electrochemical testing including cyclic voltammetry, galvanic charge discharge and cyclic stability are discussed.

Conclusion

In present work, composites of ternary metal oxide MNC and MNC with GNP were successfully synthesized through a simple, facile and cost effective hydrothermal process and further compositional, morphological and electrochemical properties were investigated. XRD was performed for the study of crystal structure and it confirmed the formation of the composite with average crystallite size ranging between 8.60-9.30 nm. SEM was performed for detailed study of microstructural properties which showed hierarchical dendritic plant like structures. These dendritic structures are low in density in MNC but later showed densly packed distict hierarchical dendritic structures by the addition of graphene nanoplatelets in MNC-GNP. Electrochemical characterization was done through VSP biological workstation in a three electrode system. Electrochemical results revealed that the synthesized material possess good supercapacitive behavior due to well-arranged morphology and synergistic contributions of individual components. MNC-GNP composite showed the high capacitance of 1816 Fg^{-1} which is higher than MNC synthesized through the same route. MNC-GNP showed higher charge discharge time than its synthesized counterpart. Moreover, material exhibited good cyclic stability with 99.5% capacity retention up to 1000 cycles. Superior electrochemical properties of MNC-GNP composite synthesized through easy hydrothermal route, proves it to be a promising electrode material for modern-day supercapacitors.

References

[1]. S. T. Glassmeyer *et al, Science of the Total Environment* 581–582 (**2017**) 909–922.

[2]. A.S. Arico, P. Bruce, B. Scrosati, J.-M. Tarascon, W. Van Schalkwijk, , J.World Scientific (**2011**) 148-159.

[3]. G. Boyle, J.Renewable Energy (**2004**) 456.

[4]. A. Yu, V. Chabot, J. Zhang, CRC press, **2013.**

[5]. J.P. Barton, D.G. Infield, J.IEEE transactions on energy conversion 19 **(2004)** 441-448.

[6]. S. Cavaliere, S. Subianto, I. Savych, D.J. Jones, J. Rozière, J.Energy & Environmental Science 4 (**2011**) 4761-4785.

[7]. W. Li, J. Liu, D. Zhao, J.Nature Reviews Materials 1 (2016) 16023.

[8]. J.W. Lee, A.S. Hall, J.-D. Kim, T.E. Mallouk, J.Chemistry of Materials 24 (**2012**) 1158-1164.

[9]. B. K. Kim, S. Sy, A. Yu, and J. Zhang, J.*Handbook of Clean Energy Systems* (2015) 1–25, **2015.**

[10]. S. R. Shanmugam, S. Adhikari, and R. Shakya, *Bioresource Technology*, **2017**.

[11]. A. K. Sani, R. M. Singh, T. Amis, and I. Cavarretta, *Renewable and Sustainable Energy Reviews* 106 (**2019**) 54–78**.**

[12]. N. M. Bahadur, T. Furusawa, M. Sato, F. Kurayama, and N. Suzuki, *Materials Research Bulletin* 45 (**2010**) 1383–1388.

[13]. K. H. Ko, Y. C. Lee, and Y. J. Jung, *Journal of Colloid and Interface Science*, 283 (**2005)** 482–487.

[14]. P. Gebraad, J. J. Thomas, A. Ning, P. Fleming, and K. Dykes **2016.**

[15]. C. S. A. Sluiter, B. Hames, R. Ruiz, J. Slui, and and D. C. ter, D. Templeton, *Technical Report NREL (2008)* 1–15.

[16]. G. W. Huber, S. Iborra, and A. Corma, J.*Chemical Reviews* 106 (**2006**) 4044–4098**.**

[17]. G. Alva, Y. Lin, and G. Fang, J. *Energy* 144 (**2018**) 341–378.

[18]. A. González, E. Goikolea, J. A. Barrena, and R. Mysyk, J.*Renewable and Sustainable Energy Reviews* 58 (**2016**) 1189–1206.

[19]. J. C. D. J. P. L.-M. S. &. C. C. M. Barbosa, J.*Membranes*, **2018.**

[20]. B. K. Kim, S. Sy, A. Yu, and J. Zhang, J.*Handbook of Clean Energy Systems* (**2015**)1–25.

[21]. J. Xu, L. Gao, J. Cao, W. Wang, and Z. Chen, J.*Electrochimica Acta* 56 (**2010**) 732–736.

[22]. S. K. Kandasamy and K. Kandasamy, J.*Journal of Inorganic and Organometallic Polymers and Materials* 28 (**2018**), 559–584.

[23]. E. E. Miller, Y. Hua, and F. H. Tezel, J.*Journal of Energy Storage* 20 (**2018**)30–40.

[24]. M. Vangari, T. Pryor, and L. Jiang, J.*Journal of Energy Engineering* 139 **(2013**) 72–79.

[25]. N. H. N. Azman, M. S. Mamat Mat Nazir, L. H. Ngee, and Y. Sulaiman, J.*International Journal of Energy Research* 42 (**2018**) 2104–2116.

[26]. N. H. N. Azman, M. S. Mamat Mat Nazir, L. H. Ngee, and Y. Sulaiman, J.*International Journal of Energy Research* 42 (**2018)** 2104–2116.

[27]. L. Kouchachvili, W. Yaïci, and E. Entchev, J.*Journal of Power Sources* 374 (**2018**) 237–248.

[28]. F. Lai, Y. E. Miao, L. Zuo, H. Lu, Y. Huang, and T. Liu, J.*Small* 12 (**2016**) 3235-44.

[29]. A. Davies and A. Yu, J.The Canadian Journal of Chemical Engineering 89 (**2011**) 1342-1357.

[30]. D. X. Kunfeng Chen, J.*Colloids and Interface Science Communications*, **2014**.

[31]. M. C. R. Kötz, J.*Electrochimica Acta*, (**2000**) 2483–2498.

[32]. Vinay Guptaa, Norio Miuraa, J.*Journal of Power Sources* **2006**.

[33]. R. Ko¨tz a, M. Carlen b, J.*Electrochimica Acta* 45 (**2000**) 2483–2498.

[34]. F. L. Ming Huang, Fan Dong,b Yu Xin Zhang, and Li Li Zhang, J. *Mater. Chem.*, **2015**.

[35]. J. C. Hao, J. *Solid State Electrochem*, **2013**.

[36]. Q.Chunzhen Yang, J.*Phys.Chem*, **2013.**

[37]. J. C. Myeongjin Kim, Ilgeun Oh and Jooheon Kim*, J.*Physical Chemistry Chemical Physics*, **2012**.

[38]. J. L. Shixiong Sun, Rutao Wang, Lingbin Kong, Xiaocheng Lia and Xingbin Yan, J. *Mater. Chem.* , **2014**.

[39]. D. C. GRAHAME, THEORY OF ELECTROCAPILLARITY, **1947**.

[40]. J. P. C. X.F.Gong, K.Y.Ma,,F.Liu, Li Zhang ,, XiaoBin, J.*Materials Chemistry and Physics* **2016.**

[41]. L. C. Jun Ge, J.*Nanoscale*, **2011.**

[42]. M. J. Kelly, "Cyclic Voltammetry," J.Journal of Chemical Education.

[43]. Iqbal, M. F., Ashiq, M. N., Iqbal, S., Bibi, N., & Parveen, B. J. *Electrochimica Acta, 246* (**2017**) 1097-1103.

[44]. M. V. S. T.C. Girija, J.Journal of Power Sources, 156 (**2006**) 705–711.

[45]. Chi-Chang Hu*, Jeng-Yan Lin, J.Electrochimica Acta 47 (**2002**).

[46]. V. K. E. Frackowiaka, K. Jurewicza, J.Journal of Power Sources 153 (**2006**) 413–418.

[47]. V. K. K. Lotaa, E. Frackowiaka, J.Journal of Physics and Chemistry **2004**.

[48]. Chou, S. L., Wang, J. Z., Chew, S. Y., Liu, H. K., & Dou, S. X. J.*Electrochemistry Communications 10* (**2008**) 1724-1727.

[49]. Laforgue, A., Simon, P., Sarrazin, C., & Fauvarque, J. F. J. *Journal of power sources 80* (**1999**) 142-148.

[50]. Dai, L., Chang, D. W., Baek, J. B., & Lu, W. J. *Small 8* (**2012**) 1130-1166.

[51]. S.R. Sivakkumara, Ji-Ae Choia, Douglas R. MacFarlane b, and D.-W. K. Maria Forsyth, J.Journal of Power Sources **,2007.**

[52]. Shin-Ming Li , Yu-Sheng Wang.Shin-Yi Yang, Chia-Hong Liu, Kuo-Hsin, J.Journal of Power Sources,**2013**.

[53]. M. C. Yunxia Huang, Zhongcheng Xiang and Yimin cui, **2018**.

[54]. A. G. Indrajit Shown, Li-Chyong Chen & Kuei-Hsien Chen, **2015**.

[55]. L. Z. Y. S. F. Z. Y. Z. J. G. C. .. &. T. J. Li, *ACS applied materials & interfaces,* **2014**.

[56]. D. A. D. Sasha Stankovich1*, Geoffrey H. B. Dommett1, Kevin M. Kohlhaas1, Eric J. Zimney1, and R. D. P. Eric A. Stach3, SonBinh T. Nguyen2 & Rodney S. Ruoff1, 442 **(2006**).

[57]. H. P. & . X. M. A. Kumar, *Procedia Engineering,* **2014**.

[58]. Huang, H. S., Chang, K. H., Suzuki, N., Yamauchi, Y., Hu, C. C., & Wu, K. C. W., *Small 9* **(2013**) 2520-2526.

[59]. A. C. R. R.K. Sharma, S.B. Desu, J. Electrochimica Acta 53 **(2008**) 7690–7695.

[60]. Y. C. Ye Hou, Tyler Hobson, and Jie Liu, J.Nano Lett**., 2010.**

[61]. D. C. GRAHAME, THEORY OF ELECTROCAPILLARITY, **1947.**

[62]. L. C. Jun Ge, J.Nanoscale, **2011.**

[63]. F. L. Encarnacion Raymundo-Piñero, and François Béguin, **2006**.

[64]. E. F. K. Kierzeka, G. Lotab, G. Gryglewicza, J. Machnikowskia, J. Electrochimica Acta **2004**.

[65]. T. M. M. Endo, T. Takeda, Y. J. Kim, K. Koshiba,H. Hara,and M. S. Dresselhausb, J. Journal of The Electrochemical Society, **2011.**

[66]. H. S. Deyang Qu , J.Journal of Power Sources **1998.**

[67]. C. P. Celine Largeot, John Chmiola, Pierre-Louis Taberna, Yury Gogotsi, and Patrice Simon, J. AM. CHEM. SOC**, 2007.**

[68]. D. H.-J. Mykola Seredycha, Gao Qing Lub, Teresa J. Bandosza, J.CARBON 46 **(2008)** 1475–1488.

[69]. M. Huang, Y. Zhang, F. Li, L. Zhang, Z. Wen, and Q. Liu, J.*Journal of Power Sources,* 252 **(2014)** 98–106.

[70]. L. &. G. H. Zhang, J.*Electrochimica Acta,* **2017**.

[71]. J. L. &. P. J. Y. Yin, J.*International journal of hydrogen energy,* **2014.**

[72]. Y. P. X. X. J. &. Y. J. Li, *Int. J. Electrochem. Sci*, 2017.

[73]. S. W. K. J. C. S. H. P. T. &. S.-H. Y. Lee, J.*ACS nano,* **2010**

[74]. X. Z. K. Z. J. S. J. &. Y. M. Li, J.*Journal of Materials Science & Technology,* **2018.**

[75]. A. K. &. R. S. Mishra, J. *The Journal of Physical Chemistry C,* **2011**.

[76]. S. L. L. H. N. H. S. M. P. A. &. H. N. M. Chiam, J.*Scientific reports*, **2018**.

[77]. H. H. C. M. L. Z. T. X. A. B. S. X. Z. .. &. M. D. Wang, J.*Nano Research*, **2012.**

[78]. A. K. S. D. K. K. M. K. &. K. G. G. Singh, J.*ACS applied materials & interfaces*, **2016**.

[79]. S. B. S. N. N. R. P. A. G. S. S. N. &. M. P. Jayasubramaniyan, J.*Journal of Alloys and Compounds*, **2019**.

[80]. Y. X. J. W. J. Y. Y. F. X. Z. S. R. &. W. C. P. Ji, J.*Journal of Power Sources*, **2018.**

[81]. C. L. B. R. Q. M. S. A. B. H. X. &. H. S. Chen, J.*Journal of Power Sources*, **2016.**

[82]. S. R. R. S. C. M. Y. Z. D. S. X. &. C. Z. Al-Rubaye, J.*Journal of Power Sources*, **2016.**

[83]. Y. M. H. H. S. Z. X. X. M. T. Y. &. M. Z. F. Zhao, J.*ACS applied materials & interfaces*, **2016**

[84]. L. C. D. D. Y. F. S. W. Z. L. &. L. M. Huang, J.*Nano letters*, **2013.**

[85]. X. H. X. L. M. S. N. G. C. L. J. M. &. L. P. S. Wang, J.*The Journal of Physical Chemistry C*, **2012.**

[86]. L. Z. Y. S. F. Z. Y. Z. J. G. C. .. &. T. J. Li, J.*ACS applied materials & interfaces*, **2014**.

[87]. G. Zhang, T. Wang, X. Yu, H. Zhang, H. Duan, and B. Lu, J.*Nano Energy* 2 **(2013**) 586–594.

[88]. B. Warren, There is no corresponding record for this reference.

[89]. J.I. Goldstein, D.E. Newbury, J.R. Michael, N.W. Ritchie, J.H.J. Scott, D.C. Joy, Scanning electron microscopy and X-ray microanalysis, J.Springer, **2017.**

[90]. H.H. Willard, L.L. Merritt Jr, J.A. Dean, F.A. J.Settle Jr, (**1988**).

[91]. J.B. Condon, J.Elsevier, **2006**.

[92]. H.M. Rootare, C.F. Prenzlow, J.The Journal of physical chemistry, 71 **(1967)** 2733-2736.

[93]. A. Muzaffar, M.B. Ahamed, K. Deshmukh, J. Thirumalai, J.Renewable and Sustainable Energy Reviews, 101 **(2019**) 123-145.

[94]. N.K. Bakirhan, B. Uslu, S.A. Ozkan, , J.Elsevier, **(2018)** 91-141.

[95]. F. Rohrbach, H. Karadeniz, A. Erdem, M. Famulok, G. Mayer, J.Analytical biochemistry, 421 **(2012**) 454-459.

[96]. D.T. Tran, V. Vermeeren, L. Grieten, S. Wenmackers, P. Wagner, J. Pollet, K.P. Janssen, L. Michiels, J. Lammertyn, J.Biosensors and Bioelectronics 26 **(2011)** 2987-2993.

[97]. A.-E. Radi, J.L. Acero Sánchez, E. Baldrich, C.K. O'Sullivan, J.Analytical chemistry, 77 **(2005**) 6320-6323.

[98]. A. Bogomolova, E. Komarova, K. Reber, T. Gerasimov, O. Yavuz, S. Bhatt, M. Aldissi, J.Analytical Chemistry, 81 (**2009**) 3944-3949.